# THE GEOLOGY OF ANNENKOV ISLAND

*By* T. H. Pettigrew

Abstract. Apart from the brief observations made by Norwegian, German and British expeditions, no previous detailed geological studies have been made on Annenkov Island.

Annenkov Island has suffered successive periods of periglacial and glacial erosion with associated changes in sea-level modifying the coastal areas. The resultant physiographic features are tentatively correlated with corresponding ones developed on South Georgia.

Large- and small-scale faulting associated with tilting are the only structural elements that have affected the rocks of Annenkov Island and adjacent Hauge Reef.

The sedimentary rocks are included in one formation which is divided into two members. The lower member is a fossiliferous thin-bedded sequence of tuffs and tuffaceous mudstones over 860 m thick and is overlain by the upper member, over 1 000 m of poorly fossiliferous volcaniclastic breccias and sandstones. The lithology, sedimentary structures and petrography of each member suggest that both sequences were deposited in a shelf environment, bordering an active volcanic arc. Laumontite, which occurs in rocks of both members, is indicative of zeolite-facies metamorphism.

The igneous rocks are divided into basic (spilitic) and intermediate assemblages. On the basis of their petrography the spilites can be subdivided into three types, whilst the intermediate assemblage consists of andesite, quartz-microdiorite and quartz-diorite intrusions which crop out on Annenkov Island, Hauge Reef and the Pickersgill Islands, respectively.

The sedimentary and igneous rocks exposed on Annenkov Island and South Georgia probably represent volcanic island-arc and marginal ocean-basin assemblages which can be correlated with similar assemblages of Upper Jurassic–Lower Cretaceous age in southern South America.

A detailed geological survey of Annenkov Island (lat. 54°29′S, long. 37°05′W; Figs 1 and 2) was undertaken during the austral summer of 1972–73 and included brief landings on two of the islands of the adjacent Hauge Reef.

Previous geological exploration of Annenkov Island had been confined to landings on the north-eastern coast by the Norwegian and German expeditions to South Georgia in the period 1927–29 (Holtedahl, 1929; Kohl-Larsen, 1930; Wilckens, 1932, 1937, 1947), and latterly by the British South Georgia Survey expeditions during which Trendall visited the island in March 1954 (Trendall, 1959).

The geology and physiography of Annenkov Island are related to those of nearby South Georgia; together they constitute part of the same continental block on the northern limb of the Scotia Ridge (Barker and Griffiths, 1972).

## Physiography

Like nearby South Georgia, Annenkov Island is situated within a periglacial regime and its topography is constantly being modified by periglacial erosion and solifluction. At present there [are] no glaciers on Annenkov Island but two earlier generations of glacial features can be recognized (Table I). The broad valleys and intervening degraded ridges of the island were probably scoured out by a large-scale glacierization, possibly correlated with the 10 000 year B.P. ice-cap glaciation of South Georgia (Clapperton, 1971). At the south-eastern end of the island there is a distinct bench above a cirque now partially occupied by Fan Lake. This cirque has been cut into a larger older basin dating from the first glacial phase. The newer cirque has a distinct lip, beyond which glacial till is patchily exposed in a stream section (station M.1175; Fig. 2). This is the only feature indicating a second less extensive glacial phase which can possibly be correlated with the 5 500 year B.P. glacierization of South Georgia (Clapperton, 1971).

Isolated remnants of a wave-cut platform 30 m above sea-level are developed along the north-eastern coast and they appear to correspond in height to the three flat-topped islands of Hauge Reef. This level of marine erosion can be correlated with the 25–50 m platforms on the north-eastern coast of South Georgia (Stone, 1974). It has been suggested that the latter were formed

TABLE I. A TENTATIVE CORRELATION BETWEEN THE GLACIAL AND MARINE GEOMORPHOLOGICAL FEATURES OF ANNENKOV ISLAND AND THOSE OF SOUTH GEORGIA

| Age | *South Georgia* | | *Annenkov Island* | |
|---|---|---|---|---|
| | *Glacial features* | *Raised beaches and marine platforms* | *Glacial features* | *Raised beaches and marine platforms* |
| | Continuing retreat of all glaciers | ? Continuing isostatic uplift. Present-day wave-cut platform. Raised beaches 1.5—2.5 m a.s.l. | | ? Continuing isostatic uplift. Present-day wave-cut platform. Extension of present-day beaches 1–2 m a.s.l. |
| A.D. 1800–1930 | Local re-advances | Raised beaches 3.5–7.4 m a.s.l. | | |
| 5 500 year B.P. (maximum advance) | Glacierization | | ? Local glacierization. Formation of small cirque with associated glacial till at Fan Lake | |
| | | 25 m wave-cut platform. Continuing fall in sea-level due to isostatic re-adjustment ↑ 50 m wave-cut platform | | 30 m dissected marine platform of Annenkov Island and Hauge Reef |
| +10 000 year B.P. (maximum advance) | Ice-cap glaciation | Piedmont glacier responsible for scouring of existing foreland areas 20–150 m a.s.l. | ? Large-scale glaciation and consequent formation of main ridges and valleys | |

Information compiled from Adie (1964), Clapperton (1971), Skidmore (1972) and Stone (1974).

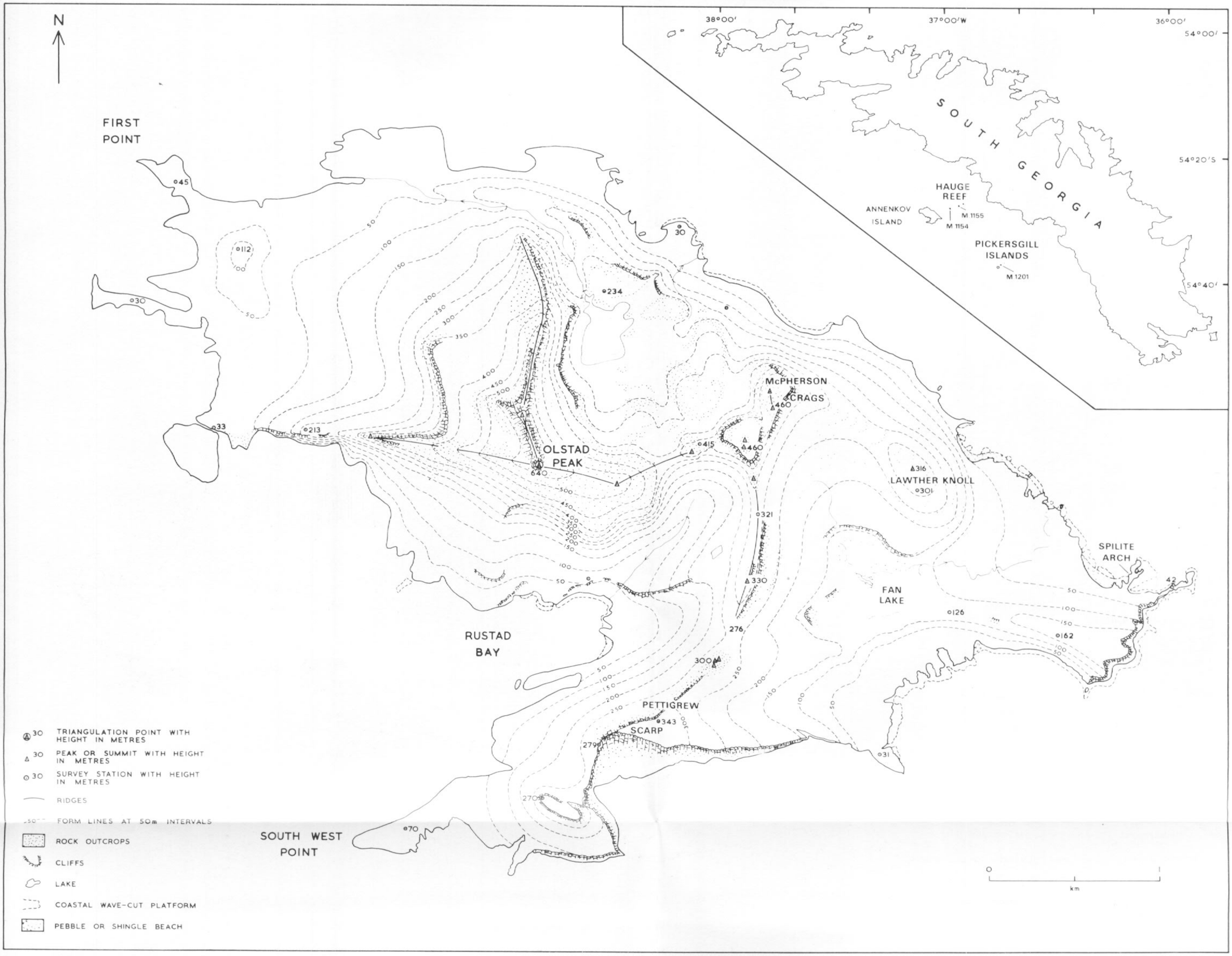


Fig. 1. Map showing the physiography of Annenkov Island.

[face page 214

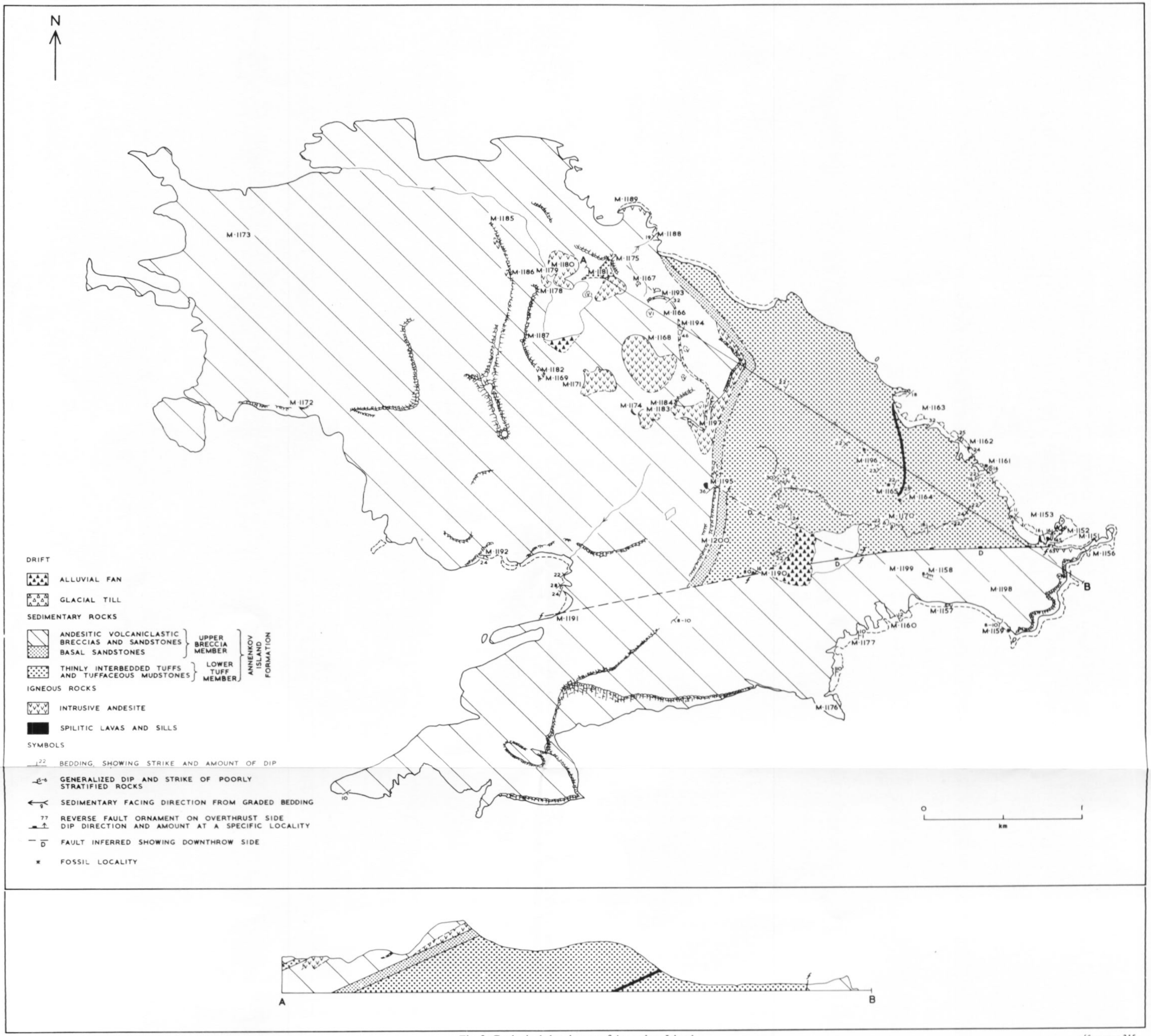


Fig. 2. Geological sketch map of Annenkov Island.

during a eustatic rise in sea-level as the Antarctic ice sheet of the 10 000 year B.P. glaciation wasted, the increase in sea-level temporarily outstripping isostatic re-adjustment of the island in response to a decreasing ice load (Stone, 1974, p. 35).

Using observations made by Rustad, Holtedahl (1929, p. 69) noted a discontinuous intertidal "wave-cut" foreland surrounding the coast of Annenkov Island. This remarkably flat platform of irregular width typically abuts directly against the cliff line. A similar platform is developed around the islets of Hauge Reef and has been recorded as a coastal feature of South Georgia (Holtedahl, 1929, p. 69; Adie, 1964, p. 28). Beach deposits overlying and occupying discontinuities in this platform often extend 1–2 m above high-water mark. These features probably indicate continuing isostatic recovery, an effect of isostatic re-adjustment after the last glacierization of the region. A tentative correlation between the physiographic features of Annenkov Island and those of South Georgia is given in Table I.

## Stratigraphy

A conformable succession of gently tilted volcanogenic sedimentary rocks at least 1 860 m thick (the Annenkov Island Formation) can be divided into two members (Table II). The lowest of these is a fossiliferous succession of tuffs and tuffaceous mudstones interpreted as a shelf facies of the Cumberland Bay Formation of South Georgia. Collections of fossils by the Norwegian and German expeditions have been described by Wilckens (1937, 1947), who considered they were of Lower Cretaceous (Upper Aptian) age. However, Casey (1961, footnote on p. 56) was of the opinion that some of the ammonites exhibited affinities with Neocomian forms. This formation is abruptly but conformably overlain by a succession of coarse structureless to poorly stratified andesitic volcaniclastic sandstones and breccias. Fossils are rare and have only been collected from one locality (Pettigrew and Willey, 1975). Large irregular intrusions of andesite are mineralogically and texturally identical to that of the andesitic clasts.

Both members contain interbedded basic (spilitic) rocks, most of which are intrusive. Quartz-microdiorite intrusions on Hauge Reef are similar in mineralogy and texture to the quartz-diorites collected from the Pickersgill Islands during a botanical survey in December 1972.

TABLE II. STRATIGRAPHY OF ANNENKOV ISLAND AND HAUGE REEF

| *Age* | | | *Sedimentary rocks* | *Igneous rocks* | *Deformation* |
|---|---|---|---|---|---|
| ? | | | | | Faulting and tilting of all rocks possibly equivalent to late-stage faulting on South Georgia |
| **Lower Cretaceous** | Annenkov Island Formation | Upper Breccia Member | At least 1 000 m of andesitic volcaniclastic breccias and subordinate sandstones with minor intercalations of mudstone | Intrusions of andesite quartz-microdiorite<br>Pillow lava | |
| | | | Volcaniclastic sandstones 91 m thick | | |
| | | Lower Tuff Member | A succession of interbedded tuffaceous mudstones, tuffs and diagenetic limestones at least 860 m thick | Spilites | |

## Structure and Metamorphism

The structure of Annenkov Island is relatively simple and, apart from localized folding and fracturing associated with large-scale faulting, the rocks have suffered no tectonic deformation. No cleavage or other tectonically induced fabrics have been developed in any of the rock types. The most significant structural feature is a major high-angle reverse fault trending across the south-eastern end of the island from the north-eastern coast to Rustad Bay. North of this fault and over most of the island, the sedimentary rocks dip fairly consistently at 20–25° to the north-west, whereas on the southern side the dip is predominantly 10–12° to the south-east. Rocks of the Upper Breccia Member have been down-faulted on the southern side of the fault against the underlying Lower Tuff Member. At station M.1152, this fault must have a minimum vertical displacement of 860 m. (This is the measured thickness of the Lower Tuff Member between the fault and the overlying Upper Breccia Member.) Whereas the thin-bedded tuffs and tuffaceous mudstones exhibit intense monoclinal and small-scale faulting in the vicinity of the major structure, an andesite intrusion within the Upper Breccia Member adjacent to the fault plane at station M.1152 exhibits no deformation apart from localized fracturing (Fig. 3).

Small-scale faulting is common in rocks of the Lower Tuff Member, especially at station M.1163 where a suite of spilitic sills has been down-faulted to the south by five faults trending at 307°, 297°, 297°, 297° and 263°, respectively.

### *Age of the faulting*

Although the Annenkov Island rocks were unaffected by the period of intense polyphase deformation which resulted in the complex tectonic features of the rocks on South Georgia, the tilting and faulting can possibly be correlated with later periods of brittle deformation responsible for the widespread and often large-scale faulting of the rocks on South Georgia.

Both members of the Annenkov Island Formation exhibit a widespread development of authigenic zeolite. An X-ray diffraction examination of a zeolitized vitric tuff confirmed an optical identification that the zeolite is laumontite associated with subordinate quartz. The occurrence of laumontite indicates that the rocks of Annenkov Island have undergone low-grade zeolite-facies metamorphism.

## Sedimentary Rocks: the Annenkov Island Formation

The sedimentary rocks of Annenkov Island and Hauge Reef consist almost entirely of the volcaniclastic products of contemporaneous intermediate volcanicity and, as such, they form a lithofacies distinct from the turbidites of South Georgia. It is proposed to designate the volcanogenic sedimentary rocks of Annenkov Island as the **Annenkov Island Formation,** which can be divided into two members:

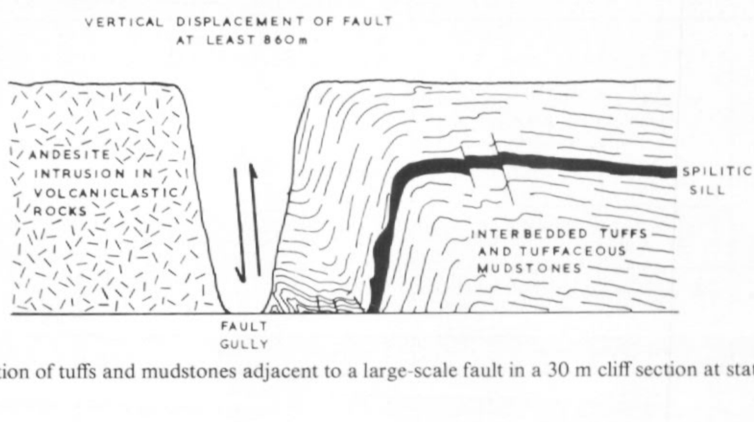


Fig. 3. Deformation of tuffs and mudstones adjacent to a large-scale fault in a 30 m cliff section at station M.1152.

i. A lower fossiliferous member consisting of thinly interbedded tuffs and tuffaceous mudstones at least 860 m thick. These rocks are well exposed on the north-eastern coast and inland on Lawther Knoll; it is proposed that this unit be named the **Lower Tuff Member.**

ii. An upper unit over 1 000 m thick and consisting of andesitic breccias and sandstones with minor intercalations of mudstone. It is proposed to name this unit the **Upper Breccia Member.**

The Annenkov Island Formation has a total thickness of at least 1 860 m.

*Lower Tuff Member*

The type sections for this member are on the north-eastern coast of Annenkov Island (M.1153, 1161, 1162 and 1163) and inland on Lawther Knoll (M.1164, 1165 and 1196). The locations of these sections are shown in Fig. 2.

The sedimentary rocks of this member were previously grouped with the Cumberland Bay Formation of South Georgia. However, the thinner bedding, predominance of mudstones, absence of sandstones with a grain-size larger than 2 mm, the fossiliferous and highly tuffaceous character of the Annenkov Island succession indicate that the latter were deposited in an environment which was marginal to the main trough of deposition in which the Cumberland Bay Formation sediments accumulated. Fossils occur sporadically throughout this member and they include miscellaneous vertebrate remains, fish, cirripedes, ammonites, bivalves, Foraminifera, Radiolaria, leaves, wood and various trace fossils. These were first described by Wilckens in 1932 and subsequently in 1937 and 1947. Trendall (1959) made the first detailed field observations on these rocks but, although he recognized that they were of a different facies, he included them in the "Cumberland Bay type" rocks of South Georgia. Rocks of this member also crop out on Hauge Reef. The locations of the sections measured are indicated in Fig. 4 and the stratigraphical succession is shown in Fig. 5. The lowest point of the succession is in faulted contact with the Upper Breccia Member (Fig. 3) and the lowermost 370 m of the stratigraphical

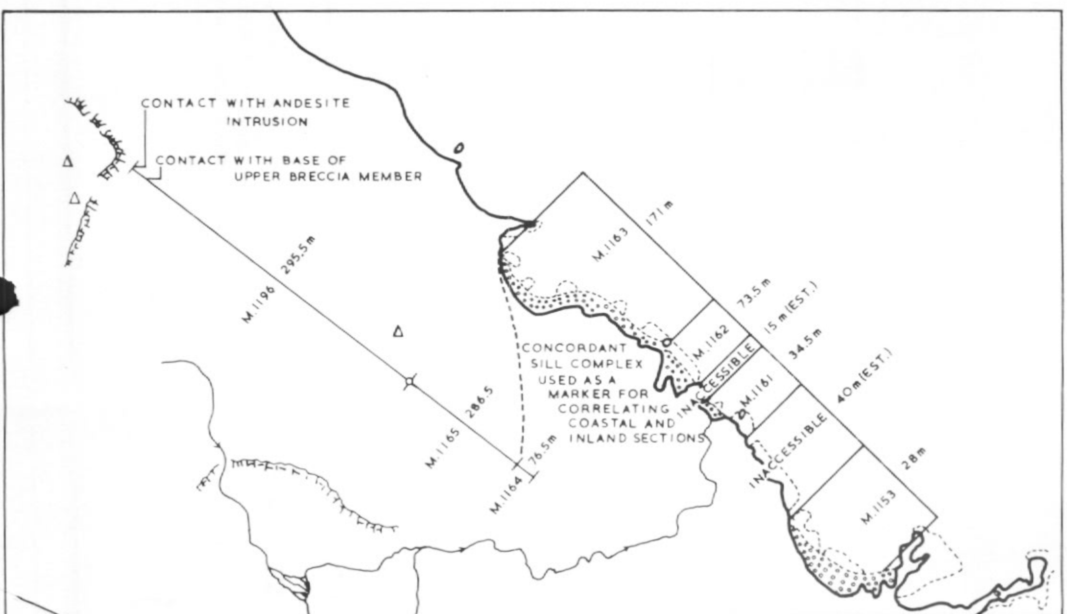


Fig. 4. Sketch map showing the locations of measured sections in the Lower Tuff Member of the Annenkov Island Formation (see Fig. 5).

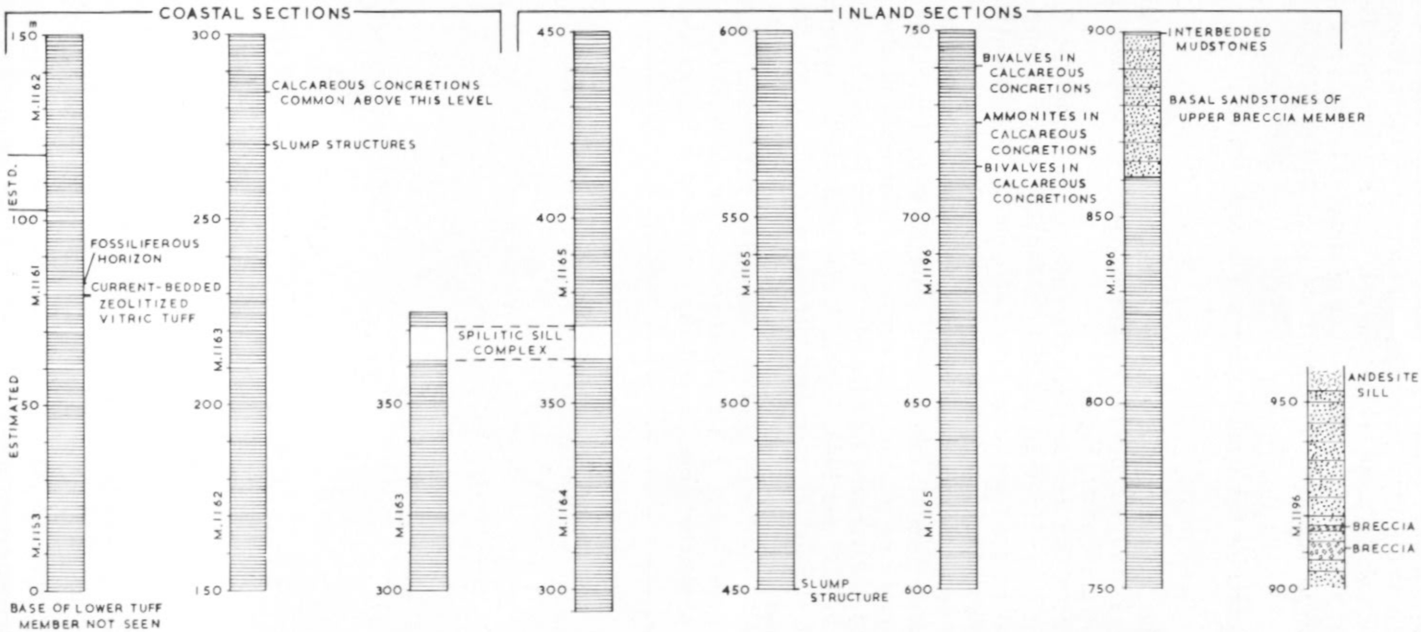


Fig. 5. The stratigraphical succession of the Lower Tuff Member up to and including the basal sandstones of the Upper Breccia Member. Vertical scale in metres; all sections were measured with a Jacobs staff and Abney level.

sequence are exposed on the shore and in cliff sections at the south-eastern end of the north-eastern coast (M.1152, 1153, 1161, 1162 and 1163). The upper 582 m are accessible inland at stations M.1164, 1165 and 1196. These coastal and inland sequences can be correlated by a concordant sill complex which is exposed at the top of the accessible coastal sequence (M.1163) and the base of the inland sequence (M.1164).

*Lithology*

Lithologically, this succession consists of a monotonous sequence of thin-bedded tuffaceous mudstones, tuffs and subordinate diagenetic limestones (Figs 6, 7 and 8b). The tuffaceous mudstones, comprising approximately 60–70% of the sequence, vary in colour from grey through grey-green to dark brown. Although individual beds are normally 1–5 cm thick, beds up to 40 cm in thickness are not uncommon. The mudstones may be uniform in appearance but more often they are thinly laminated, individual laminae varying between 0.5 and 9.0 mm in thickness. Beds and laminae of mudstone alternate irregularly with the tuffs.

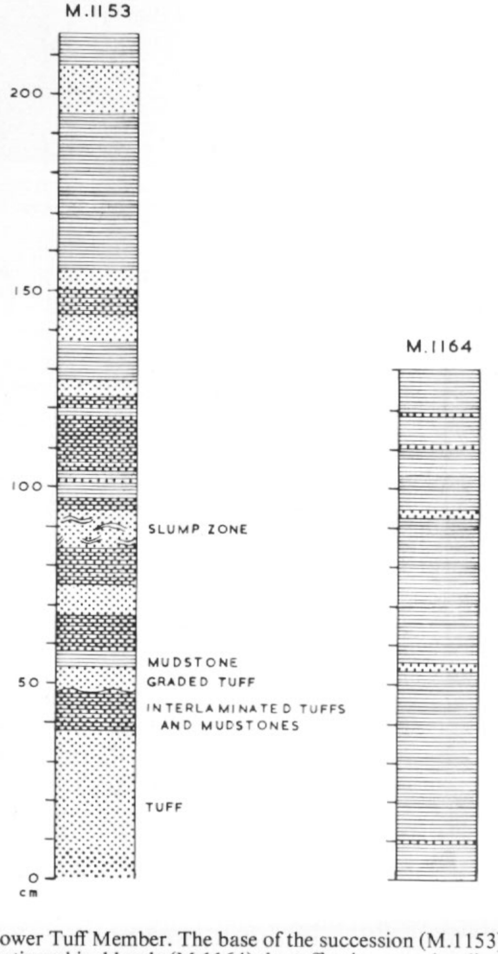


Fig. 6. Typical sections in the Lower Tuff Member. The base of the succession (M.1153) consists predominantly of tuff units, whilst at higher stratigraphical levels (M.1164) the tuff units are subordinate to mudstones. Vertical scale in centimetres.

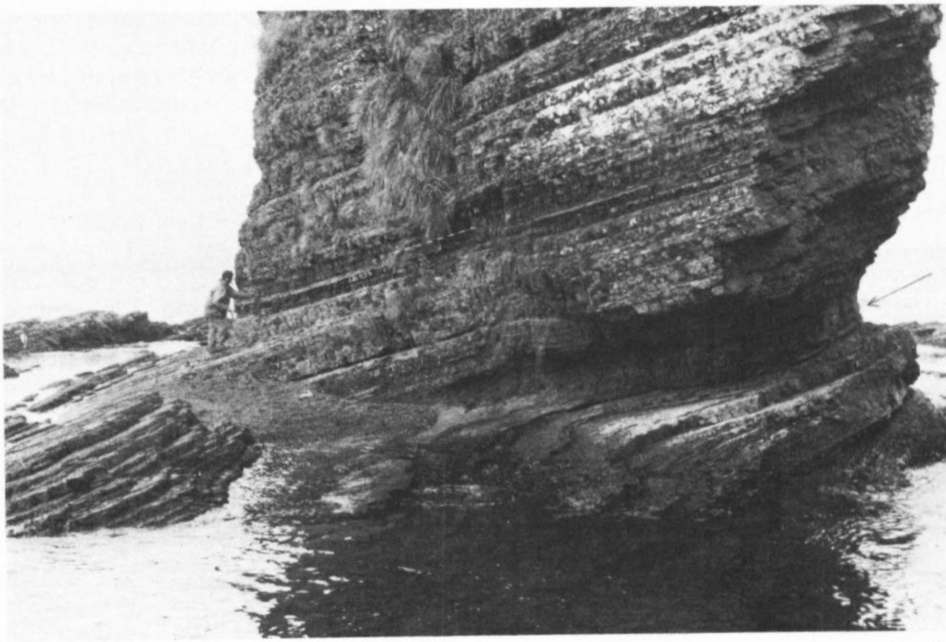

Fig. 7. Thin-bedded fossiliferous tuffs and tuffaceous mudstones dipping gently to the north-west at station M.1161. The arrow indicates the outcrop of an 18 cm thick zeolitized vitric tuff unit (see Fig. 10c and d).

A dark-coloured unlaminated mudstone collected from station M.1154 contains a pear-shaped rust-brown bleb 13 mm in length and flattened in the same plane as the bedding. This bleb, which is exceedingly thin, is also characterized by small yellow-white fragments of (?) feldspar. Volcanogenic vitric crystal blebs of a corresponding colour, size and texture to those of the Annenkov Island example have been described from the Lower Cretaceous mudstones of Alexander Island by Horne and Thomson (1972, p. 106), but the exact mode of formation of these blebs is unknown.

The tuffs are yellow to dark brown in colour, occurring in beds which are usually 3–10 cm in thickness, although units up to 2 m are present. Tuff laminae interbedded with the mudstones are rarely less than 0.03 mm in thickness.

The majority of the sedimentary rocks are calcareous and limestone occurs in the form of concretions.

*Sedimentary structures*

A high proportion of the tuff units exhibit graded bedding. These graded beds sometimes rest on an erosion surface of mudstone and occasionally they include fragments torn from the underlying mudstone. Flames of mudstone infrequently pierce the lower interfaces of the graded tuff. These features indicate deposition of some of the tuffs by small-scale turbidity currents. However, the grading in most cases can be attributed to deposition by ash falls. Whereas current-bedded tuffs were only observed at two stations, small-scale cross lamination is frequently developed in the mudstones.

A large slump structure associated with soft-sediment sliding occurs in the cliffs at station M.1163. This slump involves a zone of contorted sediments 4 m thick, whose margins are parallel to the over- and underlying undisturbed strata. Towards the base of this zone, a bed of tuff 2 m thick and 10 m long overlies more mudstones which have slumped on a plane sub-parallel to the stratification and which locally truncates the bedding. A south-south-easterly or north-northwesterly direction of movement is indicated by an overfold towards the south-south-east in the contorted strata (axial trend 253° true). Buckling associated with "slump planes" truncating the bedding occurs in a higher sequence of mudstones at this locality. These features are interpreted as soft-sediment deformational structures induced by slumping. Slump structures are developed inland at station M.1165, where movement in an east-north-east or west-south-west direction is indicated by a small overfold (axial trend 331° true).

In the cliffs at station M.1153, re-mobilization of some of the tuffs has produced remarkable structures towards the base of the succession. At one point a sequence of thin-bedded mudstones and tuffs 33 cm thick passes into a disrupted zone of non-stratification. Stringers and fragments of mudstone lie chaotically in a structureless tuffaceous matrix produced by the amalgamation of the adjacent beds of tuff. The over- and underlying sediments are normally stratified and laterally, over a distance of 2–3 m, the disrupted strata pass into a sequence of normally bedded mudstones and tuffs.

Related injection structures have developed where small-scale vertical faults locally displace the bedding. At the fault planes, the mudstone beds are sharply truncated and displaced, whereas the interbedded tuffs show no sign of brittle deformation and are connected to 1–3 cm wide "dykes" of tuff containing fragments of mudstone which are intruded along the fault planes. Another example of tuff injection along a fault plane was collected from scree at station M.1165 (Fig. 8a). Sub-surface sliding induced by slumping may have caused all these "quick-sand" structures. It is suggested that sliding caused local brecciation of the mudstone beds, while the water-saturated interbedded tuffs behaved as a fluid and formed a structureless matrix. Local faulting associated with the tuff "dykes" may have been induced by differential settling during compaction.

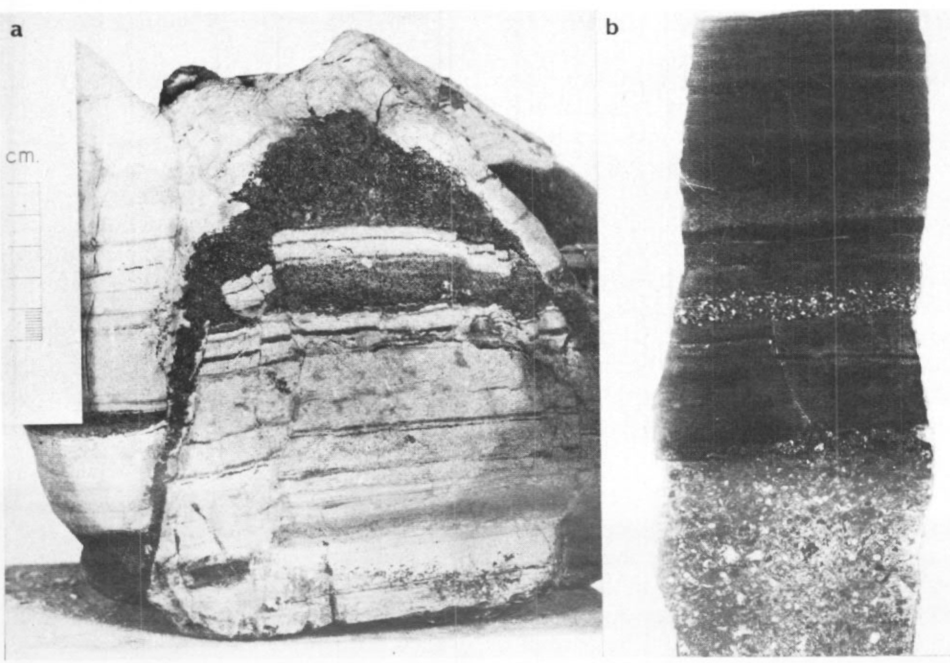


Fig. 8. a. Small-scale sedimentary dykes developed in a block of interbedded calcareous mudstones and tuffs. The tuffs are intrusive into a fault plane which has fractured the adjacent mudstones (M.1165.37).

b. Interbedded mudstones and graded tuffs from the Lower Tuff Member of the Annenkov Island Formation. Pumices are conspicuous in a calcareous vitric tuff in the lower part of the block (M.1161.40; see Figs 9a–d and 10b) (× 0.8).

Calcareous concretions occur widely in the sedimentary rocks of South Georgia and these have been previously described from the Lower Tuff Member of Annenkov Island by Trendall (1959). On Annenkov Island, the pale to blue-grey fine-grained limestone concretions are usually concentrated in definite bands parallel to, and flattened in the same plane as, the bedding. They are generally ellipsoidal but vary considerably in size and ratio of long to short axes (the long axes vary in length between 2 cm and 1.5 m, and the short axes between 1 cm and 1 m). Fossils occurring within the concretions are uncrushed and better preserved than those in the adjacent mudstones. In particular, the ammonites and trace fossils are preserved in full relief and wood has been fossilized without loss of cellular structure (Fig. 9f).

Similar concretions in Cretaceous shales in Colombia (Weeks, 1953) contain well-preserved ammonites and fish. The Lower Cretaceous sediments of Alexander Island also contain calcareous concretions (Horne and Taylor, 1969).

The stratification, which in some cases can be seen to pass through the concretions, and the bending of over- and underlying strata around them in response to compaction suggest that the concretions were formed early in diagenesis but prior to compaction. Both Weeks (1953) and Trendall (1959) reached a similar conclusion.

*Petrography*

*Tuffaceous mudstones*. The mudstones contain a variable amount of microscopic pyroclastic material which may be disseminated throughout a particular bed or unit as well as being concentrated in thin laminae (0.03–1.0 mm thick). Foraminifera occur rarely (Fig. 9b) but Radiolaria, 0.02–0.3 mm in size, are abundant, usually appearing as globular to conical patches of clear recrystallized calcite (Fig. 9a). Sometimes, however, the reticulate structure of the test is preserved and the joints and corresponding strictures separating the segments are visible in longitudinal sections of the conical varieties (Fig. 9c and d). The matrix of the mudstones may be either siliceous or calcareous.

The pyroclastic material is ashy, consisting largely of vitric (recrystallized) shards with variable proportions of crystal (feldspathic) and lithic fragments. Shards tend to predominate over the other constituents in the rocks as a whole, while variable proportions of pumice, glassy rock fragments and crystals are concentrated in the laminae. The shards vary in size from a fine dust up to fragments 0.1 mm in size. Crescentic, cuspate and Y-shaped shards are particularly common as are frothy pumice fragments with discrete spherical bubbles but attenuated long-tube pumice occurs less frequently. Pale green fragments of clinopyroxene (0.1 mm) occur sparingly. Lava fragments, represented by angular glassy greenish brown rock fragments (0.06–0.1 mm), often contain aligned microphenocrysts of oligoclase.

The matrix of the calcareous mudstones consists of a mosaic of microcrystalline calcite identical in texture to that of the calcareous concretions described above. The non-calcareous mudstones are indurated siliceous rocks but otherwise they are similar to their calcareous counterparts.

*Tuffs*. Tuff units, frequently graded, are interbedded at irregular intervals with the mudstones. The framework minerals (Nanz, 1954, p. 108) consist predominantly of fragmented plagioclase euhedra and volcanic rock fragments, with lesser amounts of recrystallized pumice and mafic minerals. As in the mudstones, the matrices of the tuffs may consist entirely of calcite, clay minerals or varying proportions of the two.

Specimen M.1161.40 consists of a graded calcareous tuff unit 6 mm thick, interbedded with calcareous mudstone (Fig. 8b). The base of the graded bed is irregular with individual volcanogenic grains depressing the laminae in the upper part of the underlying mudstone. The framework constituents of the tuff are predominantly angular, grading from an average grain-size of approximately 1.3 mm at the base of the unit to approximately 0.06 mm at the top.

Lava fragments constitute the bulk of the clastic material (Table III, M.1161.40) with pro-

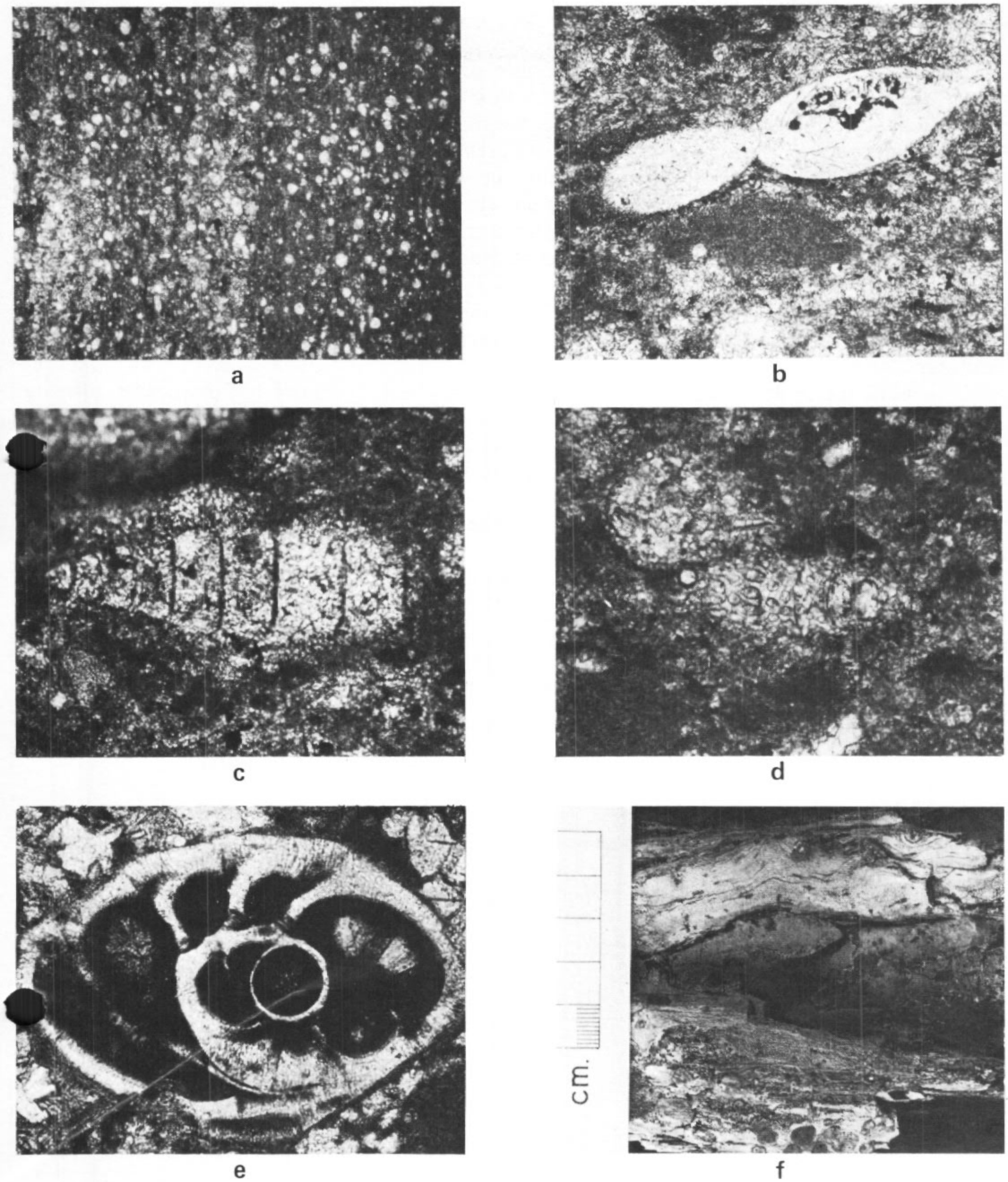


Fig. 9. a. Laminated calcareous mudstones with abundant calcified Radiolaria and rarer Foraminifera (M.1161.40; ordinary light; × 10).
b. A foram, (?) *Dentalina* sp. (M.1161.40; ordinary light; × 100).
c. A radiolarian showing joints and corresponding strictures separating the segments (M.1161.40; ordinary light; × 130).
d. A well-preserved radiolarian (M.1161.40; ordinary light; × 140).
e. A foram preserved in a tuff (M.1165.26; ordinary light; × 100).
f. Fossil wood bored by a species of (?) *Teredo* in a calcareous concretion (M.1196.15).

gressively smaller amounts of vitric and crystal (plagioclase) components. The lava fragments exhibit a variety of textures. They are generally fine-grained to glassy greenish brown amygdaloidal rocks with abundant, often flow-orientated micro- and macrophenocrysts of plagioclase (oligoclase-andesine), and pale green clinopyroxene. Plagioclase and clinopyroxene of a similar composition and appearance to the minerals recognizable in these rock fragments represent the clastic crystalline constituents of the tuff.

Devitrification of volcanic glass has resulted in some of the fragments acquiring a low-order birefringence. Thus, unless bubbles or microlites are present in such fragments, they are often extremely difficult to distinguish from feldspathic rock grains and broken plagioclase euhedra. Attenuated long-tube pumice is subordinate in amount to the spherical bubble non-attenuated type.

The matrix of the tuff is composed of interlocking crystals of anhedral calcite which often embay and partially replace some of the framework components, particularly the pumices and feldspars.

In general, the types of framework components vary little from one tuff to another, although their relative proportions vary considerably. The only exceptions (Table III, M.1153.7 and 10) were collected near the base of the exposed sequence and they differ from the other tuffs in t[illegible] they contain small amounts of apatite and quartz. In addition, the feldspars have been extensively altered to a weakly birefringent zeolite which may also have replaced the volcanic glass because no vitric material is present (cf. specimen M.1161.12 described below).

TABLE III. MODAL ANALYSES OF TUFFS AND VOLCANICLASTIC SANDSTONES FROM THE ANNENKOV ISLAND FORMATION

| | *Lower Tuff Member* | | | | | | | *Upper Breccia Member* | | | | | | |
|---|---|---|---|---|---|---|---|---|---|---|---|---|---|---|
| *Analysis number* | 1 | 2 | 3 | 4 | 5 | 6 | 7 | 8 | 9 | 10 | 11 | 12 | 13 | 14 |
| Quartz | 1.4 | 1.7 | — | — | — | — | — | — | — | — | — | — | — | — |
| K-feldspar | — | — | — | — | — | — | — | — | — | — | — | — | — | — |
| Plagioclase | 0.2 | 0.3 | 4.4 | 15.6 | 14.0 | 3.7 | 44.5 | 4.3 | 22.8 | 25.2 | 15.2 | 17.0 | 7.1 | 34.0 |
| Pyroxene and amphibole* | 2.1 | 2.1 | 0.6 | 1.0 | 0.5 | 0.5 | 0.2 | 4.5 | 9.2 | 3.4 | 4.5 | 3.9 | 4.6 | 2.2 |
| Opaque ores | 0.9 | 0.7 | 0.7 | 0.4 | 0.5 | 0.8 | 2.7 | 2.6 | 3.0 | 3.5 | 3.8 | 6.6 | 3.0 | 3.0 |
| Apatite | 0.2 | — | — | — | — | — | — | 0.2 | 0.1 | 0.3 | 0.3 | 0.1 | 0.1 | — |
| Lava fragments | 17.5 | 14.1 | 10.2 | 9.0 | 17.2 | 19.1 | 0.2 | 53.7 | 27.5 | 18.0 | 26.7 | 42.7 | 56.3 | 11.2 |
| Vitric fragments (recrystallized) | — | — | 4.6 | 15.9 | 9.0 | 6.2 | 4.9 | — | — | — | — | — | — | — |
| Calcite | 0.9 | 0.9 | 76.7 | 0.1 | 10.0 | 66.1 | 0.2 | 23.3 | — | 0.2 | 48.4 | 24.1 | 28.0 | 0.1 |
| Zeolite | 43.0 | 34.6 | — | 0.2 | 0.8 | — | 0.6 | — | 4.6 | 1.8 | — | 2.5 | 0.9 | 2.0 |
| Miscellaneous matrix | 33.6 | 45.6 | 2.8 | 57.8 | 48.0 | 3.6 | 46.7 | 1.4 | 32.8 | 45.6 | 1.1 | 3.1 | — | 47.5 |
| Total matrix (calcite + zeolite + miscellaneous matrix) | 77.5 | 81.1 | 79.5 | 58.1 | 58.8 | 69.7 | 47.5 | 24.7 | 37.4 | 47.6 | 49.5 | 29.7 | 28.9 | 49.[illegible] |
| Tuffaceous framework components recalculated to 100% | † | † | | | | | | | | | | | | |
| Vitric fragments (V) (recrystallized) | | | 24 | 38 | 22 | 21 | 10 | — | — | — | — | — | — | — |
| Crystal fragments (C) | | | 23 | 40 | 36 | 14 | 89.7 | 26 | 54 | 63 | 43 | 33 | 17 | 76 |
| Lava fragments (L) | | | 53 | 22 | 42 | 65 | 0.3 | 74 | 46 | 37 | 57 | 67 | 83 | 24 |

*Amphiboles are restricted in occurrence to the sediments of the Upper Breccia Member.
†Feldspars and matrix extensively zeolitized. Recalculated percentages are meaningless.

1. M.1153.7 Altered tuff.
2. M.1153.10 Altered tuff.
3. M.1161.40 Lithic tuff.
4. M.1165.25 Crystal-vitric-lithic tuff.
5. M.1165.26 Lithic-crystal-vitric tuff.
6. M.1196.4 Lithic tuff.
7. M.1196.7 Crystal tuff.
8. M.1188.2 Volcaniclastic sandstone.
9. M.1196.8 Volcaniclastic sandstone.
10. M.1151.6 Volcaniclastic sandstone.
11. M.1157.7 Volcaniclastic sandstone.
12. M.1159.3 Volcaniclastic sandstone.
13. M.1159.5 Volcaniclastic sandstone.
14. M.1160.2 Volcaniclastic sandstone.

Apart from the two exceptions mentioned above, the non-calcareous tuffs are broadly similar to the calcareous tuffs in their framework content. Specimen M.1165.25 (Table III) is from a non-graded tuff unit 3 cm thick and interbedded with mudstones. Volcaniclastic material, occurring as angular to sub-rounded fragments (0.06–0.5 mm), consists predominantly of devitrified vitric material (Fig. 10a) and fragmental andesine euhedra with smaller amounts of lava fragments and pyroxene. The matrix is non-calcareous and consists of clear colourless analcite interspersed with clay minerals, both of which partially replace the vitric material. Other unidentified, weakly birefringent zeolites occur as discrete interstitial patches.

In a second tuff specimen (Table III, M.1165.26), the matrix is composed of clay minerals, zeolites and calcite. The calcite occurs as interstitial anhedral crystals (0.06–0.6 mm) and is clearly secondary in origin. A notable feature is that cracks between and within the calcite crystals are often filled with clay minerals, suggesting that the calcite precipitation took place prior to the formation and introduction of the clay minerals. The significance of this is discussed later (p. 226). Well-preserved Foraminifera also occur in the tuff (Fig. 9e).

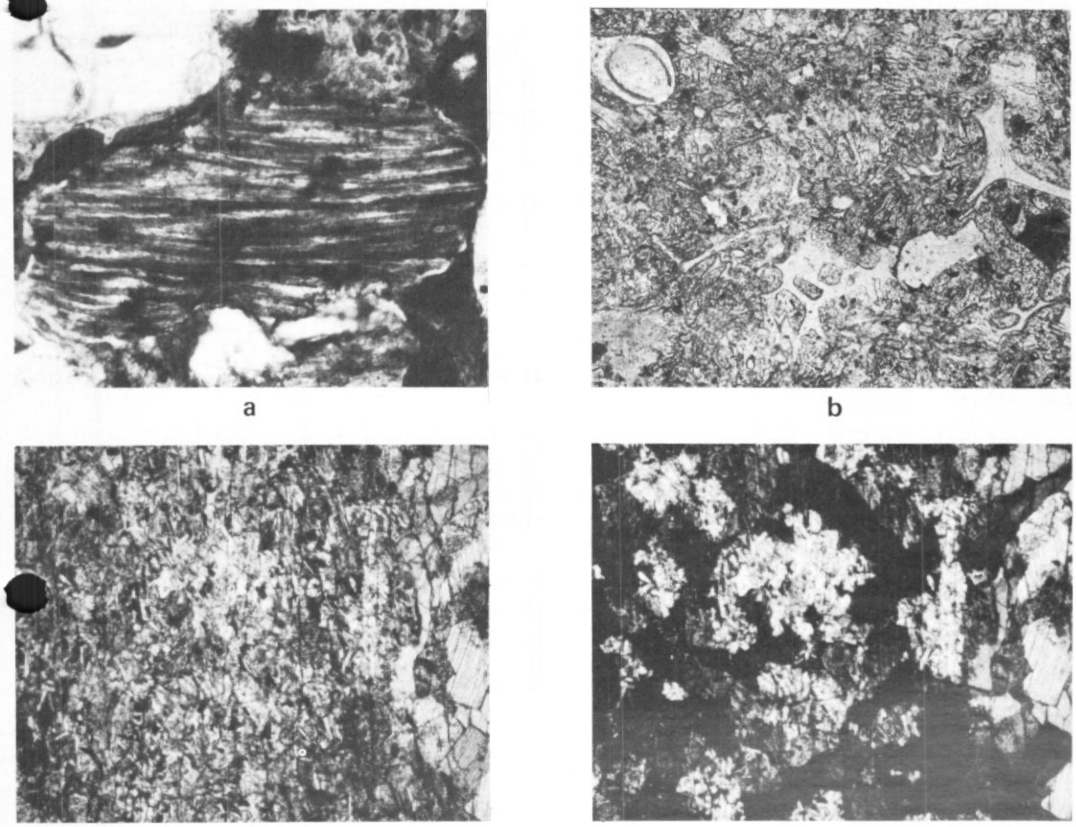

Fig. 10. a. An attenuated long-tube pumice in a tuff (M.1165.25; ordinary light; × 140).
b. Calcareous vitric tuff showing a variety of typical shard textures (M.1161.40; ordinary light; × 100).
c. Zeolitized vitric tuff with numerous relicts of original glass shards (M.1161.12; ordinary light; × 25).
d. As for Fig. 10c, but viewed under X-nicols. The tuff has been almost completely altered to an interlocking mosaic of zeolite (laumontite) crystals (× 25).

Calcareous vitric tuffs of variable thickness are interbedded with the mudstones and normal tuffs. At their thinnest they occur as laminae in the mudstones, whereas larger units are up to 18 cm in thickness.

Part of specimen M.1161.40 (Fig. 8b) consists of a calcareous vitric tuff unit 4 cm thick. Angular fragments of pumice up to 3 mm in size are particularly conspicuous. Tubular and spherical bubble pumices are strikingly displayed in thin section as are equally abundant shards (Fig. 10b). All of these clastic components, none of which show any sign of abrasion, are set in and partially replaced by a mosaic-like matrix of diagenetic calcite of crystal size 0.03–0.2 mm.

An extensively altered vitric tuff crops out in the cliffs at station M.1161 (Fig. 7). The 18 cm thick unit is unevenly stratified, creamy brown in colour and consists of a soft, friable, finely granular rock. Current bedding is developed near the base. Thin sections show that the tuff is composed of a mosaic of interlocking zeolite crystals, 0.1–0.7 mm in size, enclosing relict, predominantly linear shards. Subordinate quartz occurs with the zeolite and the whole is peppered with clay-mineral particles and opaque ores (Fig. 10c and d). The unit is interpreted as an ash fall or re-deposited ash which originally contained a high proportion of unstable volcanic glass.

A high proportion of the authigenic zeolites which are patchily but widely developed in the sedimentary rocks of both members of the Annenkov Island Formation are optically and texturally identical to the zeolite of the vitric tuff. It has thus been tentatively assumed that all of these zeolites are of a single mineral species. Taking advantage of the high concentration of the zeolite in the tuff, a finely powdered sample was prepared in an effort to identify the zeolite using an X-ray diffractometer. The resultant traces indicated the presence of laumontite associated with quartz in the sample. Laumontite is one of the principal index minerals of zeolite-facies metamorphism (Coombs, 1960). From this it can be inferred that the rocks of both members have undergone zeolite-facies metamorphism.

Similar examples of vitric tuff zeolitization have been recorded by Horne (1968, p. 6–7) from the Lower Cretaceous sediments of Alexander Island.

*Interpretation of modal analyses*

Modal analyses of seven of the tuffs collected from the Lower Tuff Member are given in Table III.

The almost complete absence of quartz and the total absence of K-feldspar* compared with the abundance of andesine and lava fragments of andesitic composition imply a calc-alkaline source for the detritus. The relative abundance of vitric material in the tuffs and associated mudstones suggests that the source of the tuffs was an active volcanic centre rather than an old volcanic terrain undergoing erosion, because this would have yielded lower proportions of vitric material than are found in the Annenkov Island tuffaceous sediments.

All the tuffs possess a high proportion of matrix, which is variable in composition. Many authors have commented on the susceptibility of immature volcaniclastic sediments to diagenesis and metamorphism (Pettijohn and others, 1972, p. 267). Two of the principal products of metamorphism are clay minerals and zeolites, both of which are present in significant amounts in some of the Annenkov Island tuffs. Cummins (1962, p. 65), Zen (1961) and Stewart (1974) considered that calcite, precipitated early in diagenesis, might form a protective coating around the framework minerals of a sandstone, thus reducing its permeability and protecting the grains against further diagenetic and metamorphic degradation. In this respect, it is interesting to note that the calcite in the carbonate concretions must have been precipitated at an early stage in

*The usual procedure of etching and staining uncovered thin sections could not be adopted in this instance as many of the sandstones possess calcareous matrices which would have been destroyed if etched with hydrofluoric acid. Therefore, to test for the presence of K-feldspar, slices of sandstone were etched and stained, each slice representing a corresponding modally analysed thin section. The slices were then varnished and examined under the microscope using reflected light.

diagenesis (before compaction). It therefore seems reasonable to suppose that the diagenetic calcite of the mudstones and tuffs was likewise precipitated at an early stage in diagenesis. Where a calcareous cement has been developed, the calcite is clear and there is no sign of a clay mineral/zeolite type matrix. Furthermore, in specimen M.1165.26 (described above) it can be demonstrated that the clay-mineral matrix exhibits an interstitial relationship to the calcitic matrix. The evidence thus suggests that the calcareous matrix was formed early in diagenesis and that subsequent metamorphism of the volcaniclastic framework minerals produced a clay mineral/zeolite matrix which was partially moulded upon the earlier calcareous cement.

Assuming that the matrix is secondary, it follows that there is no correlation between the overall proportions of framework and matrix components in the tuffs. Inaccuracies in the modal analyses arise from the selective diagenetic replacement and modification of some of the framework materials. Hence, preferential zeolitization and calcification have, in some cases, partially eliminated vitric and felsic constituents. For example, in analyses M.1153.7 and 10 (Table III), a high proportion of zeolitic matrix can be correlated with an abnormally low percentage of feldspar (replacement features are visible in the thin section) and may also be related to the complete absence of vitric material. Peripheral diagenetic modification of many of the lithic clasts has effectively disguised the clast–matrix boundary and has probably resulted in an over-estimation of the matrix.

*Upper Breccia Member*

The Lower Tuff Member is overlain by at least 1 000 m of coarse volcaniclastic breccias and subordinate sandstones. These are andesitic in composition and are closely related to associated intrusive bodies of andesite. The breccias and intrusive rocks crop out over most of Annenkov Island and are responsible for the rugged topography of the central area. It can be demonstrated that the breccias were deposited by mass-flow processes and they also exhibit most of the characteristic features of laharic breccias as defined by Fisher (1960, p. 127). They are interpreted either as original subaerial lahars which flowed from an island-arc terrain into the adjacent ocean (cf. Mitchell, 1966, 1970; Mitchell and Warden, 1971) or, more likely, as submarine slides initiated on the flanks of an active andesitic marine volcano (cf. Jones, 1967, p. 1281). Interbedded discontinuous thin sequences of mudstone indicate a periodic return to the depositional environment under which the underlying Lower Tuff Member accumulated.

The type sections of this member are in the cliffs adjacent to Olstad Peak where massive units of breccia are well exposed, between station M.1196 and McPherson Crags where the basal sandstones of the member lie conformably above the tuffs and mudstones of the Lower Tuff Member, and in the cliffs and foreshore at station M.1160 where the relationships between massive and stratified sequences are well exposed.

Apart from wood, fossils are scarce and were observed and collected at only one locality (M.1159). These consisted of belemnites (Pettigrew and Willey, 1975) associated with an indeterminate ammonite and shell fragments.

*Basal sandstones*

The only accessible exposure of the contact between the Lower Tuff Member and the overlying volcaniclastic sequence is north-west of station M.1196 on a ridge connecting Lawther Knoll with a scarp beneath McPherson Crags capped in part by an andesite sill (Figs 4, 5 and 11). The upper part of the Lower Tuff Member consists of interbedded tuffs and tuffaceous mudstones which are abruptly overlain by the basal beds of the volcaniclastic sequence: 91 m of thin- to thick-bedded volcaniclastic sandstones. These sandstones form a mappable unit at the base of the Upper Breccia Member and can be traced right across the island from the north-eastern coast (M.1188) to the area west of station M.1190 where they are faulted out.

Lithologically and petrologically, the sandstones are clearly related to other sandstone units within the overlying volcaniclastic succession. North-west of station M.1196, the complete sandstone succession of 91 m is fairly well exposed in the lower part of the scarp beneath the andesite sill (Fig. 11). Many of the sandstones contain sporadic angular clasts of andesite and tuffaceous mudstone (up to 1.5 cm in size), which are products of penecontemporaneous erosion. At least one unit of mudstone is interbedded in the sandstones and towards the top of the section there are several units of structureless breccia. These consist of sub-rounded fragments (2–3 cm) of andesite set in a sandstone matrix. The andesite sill interposes at the top of the sandstone succession and, in turn, it is patchily capped by massive volcaniclastic breccia, thus indicating that the andesite was injected along the plane of contact between sandstone and breccias. At station M.1188 the sill is missing but a sharp concordant contact between sandstones and breccias is visible (Fig. 11). Within the sandstone sequence there is a 30 cm thick intraformational breccia composed of penecontemporaneously eroded angular sandstone clasts. Similarly, at the south-western end of the outcrop the sandstones are abruptly but concordantly overlain by the massive breccias.

*Volcaniclastic breccias and sandstones*

*Unstratified breccias*. Massive unstratified breccias constitute a large proportion of the Annenkov Island Formation. Typically, they consist of angular to sub-rounded clasts of andesite, often of large size, set in an andesitic sandstone matrix. Lack of stratification, poor

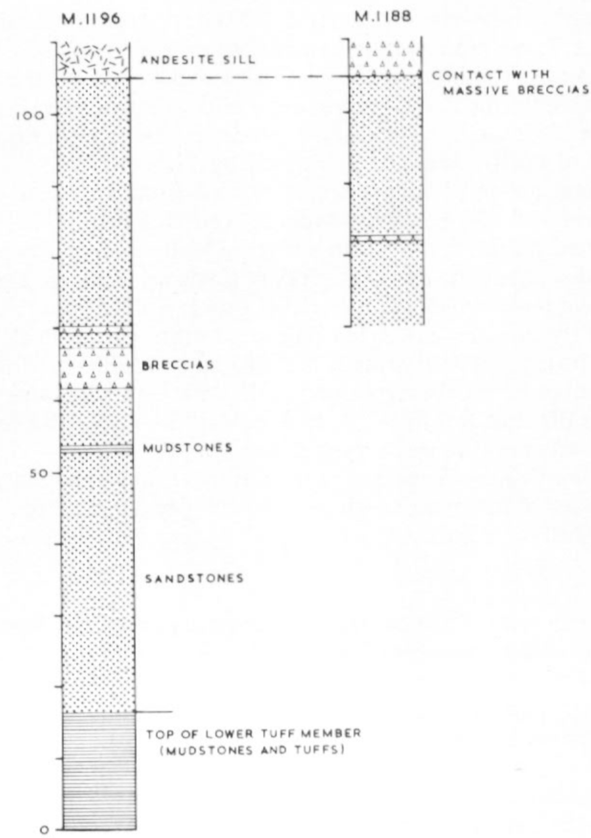


Fig. 11. Sections illustrating the change of facies from the tuffaceous sediments of the Lower Tuff Member to the sandstones and structureless breccia units of the Upper Breccia Member. Vertical scale in metres.

sorting and irregular basal erosion surfaces suggest that the breccias were deposited by mass-flow processes. The cliffs at station M.1151 expose a succession of the breccias at least 40 m thick consisting of angular to sub-rounded fragments 1 cm to 1 m in size (Fig. 12). The andesitic clasts are predominantly porphyritic and many have flow-orientated phenocrysts. In addition to the andesitic clastic material, large irregular blocks of volcaniclastic sandstone and pebbly sandstone are incorporated within the breccias and have probably been penecontemporaneously eroded from previously deposited sediments. Several localized examples of graded bedding in the breccias were observed but it is difficult to determine whether these are primary sedimentary features which have been partially obliterated by subsequent sedimentation or whether they represent penecontemporaneously derived blocks of sediment.

*Bedded breccias and sandstones.* In the cliffs south of Pettigrew Scarp, where the volcaniclastic rocks reach their most spectacular development, there is an unbroken succession (over 200 m thick) of numerous structureless breccia units producing a crude large-scale stratification (Fig. 13). The "bedded" breccias are lithologically identical to their unstratified counterparts and similarly possess a sandstone matrix. Other stratified sequences consist of interbedded structureless breccias and sandstones. Typically, there are no sharply defined bedding planes in such sequences and only the proportion of coarse clastic material fluctuates. Hence, it is the sudden appearance or disappearance of coarse clastic material within an otherwise continuous sequence of sandstone grade which defines both lithology and stratification. All gradations between sandstones, pebbly sandstone through to breccia may occur in these stratified exposures (cf. Jones, 1967, p. 1282–83). Some of the breccia units contain a high proportion of well-rounded pebbles and cobbles mixed in with the angular phenoclasts.

Generally, the stratified sequences tend to be localized and they frequently merge laterally and vertically into unstratified breccias.

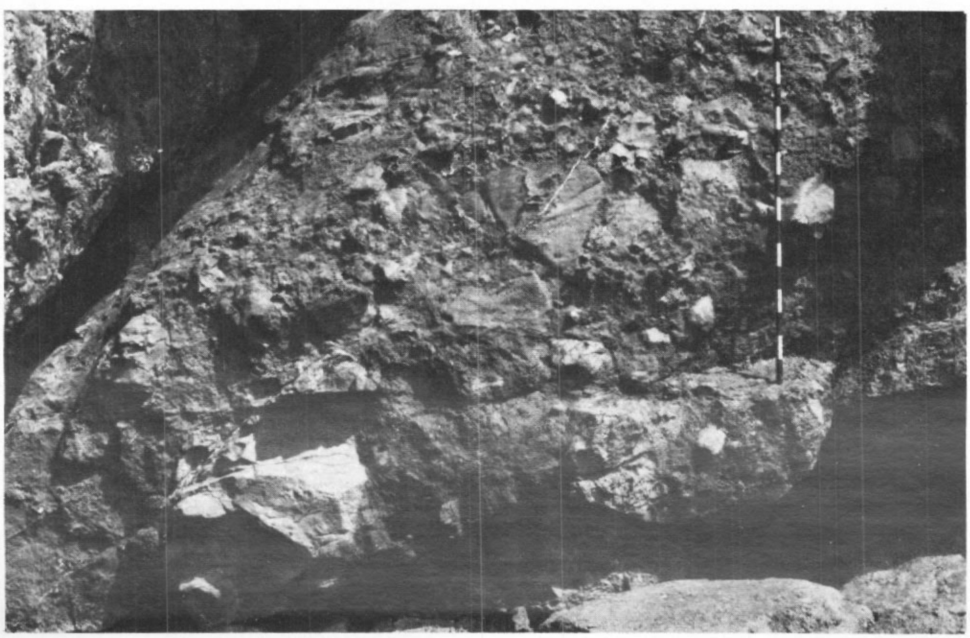

Fig. 12. Part of a massive unit of structureless volcaniclastic breccia at station M.1151. The staff is graduated in 10 cm units.

Fig. 13. A 200 m thick succession of structureless volcaniclastic breccia units exposed on the south coast of Annenkov Island, south of Pettigrew Scarp.

A variety of sedimentary structures is displayed in an 11 m stratified sequence of breccias and sandstones exposed in low cliffs and on the foreshore at station M.1160. Within this succession, a deposit of thin-bedded sandstone, 1.6 m in maximum thickness, exhibits large-scale cross bedding. This sandstone, which is also characterized by thin siltstone laminae (2–5 mm), is lithologically unique within the Upper Breccia Member. The overall lensoid shape of the unit suggests that it may represent a deposit infilling a channel cut in the underlying unit of structureless breccia. A 25 cm graded bed of breccia overlies the sandstone unit, on an erosional contact, and in turn this is succeeded by 6–7 m of structureless breccias with thin discontinuous sandstone units. A cliff section adjacent to these exposures demonstrates the lateral discontinuity of the previously described lithologies and exposes a clearly stratified sequence of relatively thick interbedded units of pebbly sandstone and structureless breccia. A 5–6 m thick unit of structureless breccia overlies an eroded surface on the underlying stratified sequence, the upper units of which have been buckled and disrupted by traction as the overlying breccia was deposited (Fig. 14).

*Interbedded mudstones*. Mudstones similar to those of the Lower Tuff Member are sometimes interbedded with breccias in the Upper Breccia Member. The units of mudstone, which vary between 2 and 10 m in thickness, tend to be laterally discontinuous and exhibit erosional contacts with the overlying breccias. One such unit exposed at station M.1181 consists of thin-bedded mudstones (2–3 cm), which, near the erosional contact with the breccias, show consistent slump overfolding towards the north. Small angular fragments of mudstone are incorporated within the breccia immediately overlying the contact.

At station M.1193 another mudstone sequence crops out and, after wedging out completely southward, it re-appears 20 m away at station M.1194 from whence it can be traced laterally for a further 800 m before it finally disappears near station M.1183 (Fig. 2). At stations M.1193 and 1194, where the mudstones are best exposed, they vary in total thickness from 3 to 10 m and calcareous concretions 1–2 m long are developed. As at station M.1181, the upper contact of the mudstone unit with the overlying breccias is erosional and large blocks and elongated twisted slabs of mudstone, up to 4 m in size, are included within the overlying breccia (Fig. 15). These derived mudstone masses, together with the upper part of the *in situ* mudstone sequence, exhibit slump folding. At station M.1193 the slump-folded upper part of the *in situ* mudstone unit contains discontinuous lensoid masses of structureless breccia up to 1 m in thickness. At station M.1194, where the upper part of the mudstone sequence is least disturbed, the lensoid masses of

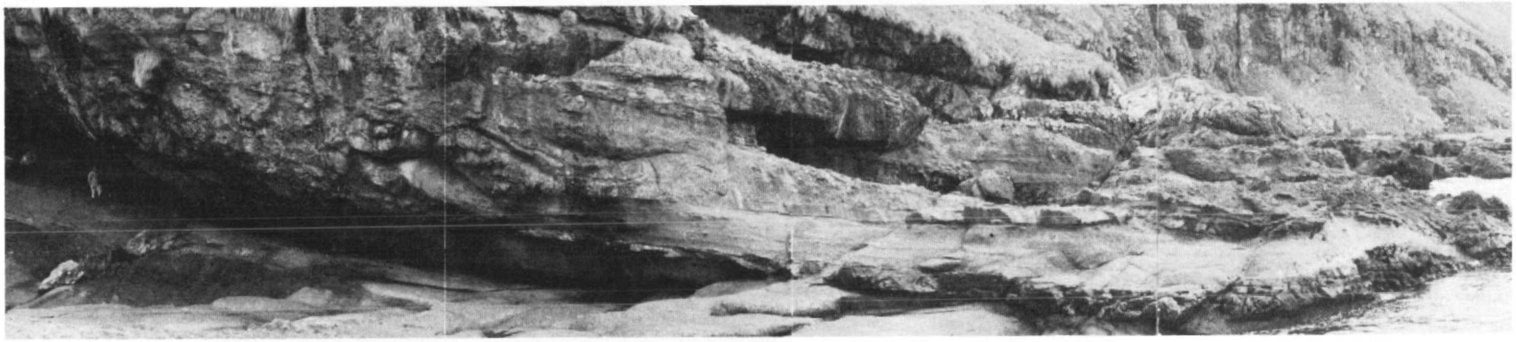

Fig. 14. Cliff and foreshore sections exposing a succession of interbedded breccias and sandstones. A massive unit of structureless breccia towards the top of the section, and well exposed in the low cliff on the left-hand side of the photograph, rests on an erosion surface of stratified rocks which have been severely ruckled near the contact with the massive unit (M.1160).


Fig. 15. A unit of structureless breccia overlying an erosion surface on thin-bedded mudstones. Large slump-folded rafts of the mudstone have been incorporated into the breccia which is at least 10 m thick. (From a photograph and field sketch; M.1193.)

breccia are represented by a thin (0.5 m) undisturbed bed of breccia within the mudstone sequence.

All the soft-sediment deformation and erosion exhibited by units within the Upper Breccia Member can be attributed to scouring and sudden mass loading associated with the movement and deposition of submarine mud flows. The source and the cause of the mass-flow processes involved are discussed later (p. 235).

*Petrography*

Sandstones and breccias throughout the Upper Breccia Member exhibit little variation in composition (Table III). Typically, the clastic material consists of largely unaltered andesitic rocks and minerals with subordinate amounts of dacite and microdiorite. Significant features are the absence of K-feldspar and pumice. Absence of the latter is probably the reason for the smaller proportion of diagenetic matrix (especially zeolite) in the sandstones in comparison with the tuffs of the Lower Tuff Member. Secondary calcite is the predominant matrix material, although matrices of clay minerals and comminuted mineral fragments also occur.

The lithic clastic material varies from sandstone grade to boulders and blocks of over 1 m in size. Nearly all of the andesitic clasts are strongly porphyritic, containing phenocrysts of zoned plagioclase, pyroxene and amphibole. Commonly, these phenocrysts are flow orientated.

The plagioclase phenocrysts, which are typically 0.03–2.0 mm in length, often exhibit oscillatory and compositional zoning from a calcic (labradoritic) core to a sodic rim of oligoclase. They are generally subhedral to euhedral, fresh and unaltered (Fig. 18a). However, feldspars in some of the andesites show patchy sericitization and zeolitization, whilst others possess recrystallized cores and contain small blebs of chloritic material. Pale green anhedral to euhedral phenocrysts (0.06–1.5 mm) and crystal aggregates of fresh augite characterize most of the andesites. Amphibole phenocrysts are of more sporadic occurrence and are absent from many of the pyroxene-andesites. Where present, they occur in the form of subhedral to euhedral crystals often exhibiting marginal to total replacement by magnetite (Fig. 18b). They vary in size from 0.03 to 3.0 mm and are of two varieties: common hornblende and lamprobolite (= basaltic hornblende). The two types are often developed within the same crystal, suggesting an inversion relationship.

Accessory minerals in the andesites include relatively large subhedral to euhedral crystals of apatite and magnetite, which may occur either in aggregates or as a fine granular dust pervading the groundmass. A few of the andesites are amygdaloidal, the amygdales consisting of chlorite, zeolite or calcite. The andesite matrices vary from glassy (devitrified) to microcrystalline. Often they show patchy zeolitization and are rich in disseminated haematite, which imparts a rich red colour in transmitted and reflected light.

Dacitic fragments occur less frequently than the andesitic clasts and consist almost entirely of strongly zoned plagioclase phenocrysts (0.1–3.0 mm in length) set in a granular groundmass of quartz intergrown with plagioclase. Although completely altered, rare mafic phenocrysts in the dacites are identifiable by their crystal shape as pseudomorphs after amphibole (probably hornblende). Infrequent, patchy zeolitization and haematitization of the groundmass is similar to that exhibited by the andesites.

Only two non-volcanic clasts were observed. The first is a large rounded boulder of coarse-grained hornblende-gabbro collected from the shore section at station M.1192. In thin section it is extremely fresh and consists of equigranular interlocking crystals of labradorite ($An_{60}$), pale green augite (identical to that within associated pyroxene-andesite clasts) and common hornblende. The relative proportion of hornblende to augite is difficult to estimate but it appears that the hornblende is subordinate in amount to the augite. Small optically continuous blebs of augite sometimes occur within the hornblende crystals. the accessory minerals include large (1.3 mm) biaxial apatites, which are similar in crystal form and development to the apatites in the andesitic clasts. An opaque iron ore occurs as coarse granular aggregates. The gabbro boulder is probably a cognate xenolith erupted with related volcanic products.

The second clast, a pebble of chert, is the only non-igneous rock fragment (with the exception of penecontemporaneously eroded sediments) collected from the breccias. This may have been incorporated from wall rock during volcanic eruption.

The clastic mineralogy of the breccias is directly related to the mineral content of the lava fragments and consists of euhedral to anhedral fragments of zoned plagioclases, pyroxenes, amphiboles, apatites and magnetites. Although quartz was not recorded during the modal analyses, several grains were observed during examination of the sandstones.

Most of the sandstones possess a secondary calcareous cement identical in character to that developed in the tuffs of the Lower Tuff Member. Other matrix minerals consist of phyllosilicates and comminuted mineral particles with subordinate patches of zeolite. Some of these matrices are identical in appearance to the fine-grained matrices of the included andesitic clasts.

*Comparison with the tuffs of the Lower Tuff Member*

The modal analyses of seven sandstones collected from the Upper Breccia Member (Table III) were obtained by exactly the same procedure as that adopted for the analyses of the Lower Tuff Member. The mafic and felsic mineralogy of both tuffs and sandstones is consistent with their derivation from a calc-alkaline volcanic source. However, the absence of pumiceous material (with a correspondingly lower proportion of zeolite) from the rocks of the Upper Breccia Member compared with the abundance of pumice in the Lower Tuff Member indicates that, whereas the clastic material of the latter was produced by explosive volcanic eruption of vesiculating magmas, vesiculation was suppressed during the formation of the clastic material comprising the Upper Breccia Member. The abundance of coarse clastic material and heavy minerals such as apatite, pyroxene and amphibole indicates a local source for the components of the Upper Breccia Member. Possible modes of deposition of the two sedimentary sequences are discussed below.

The unusual modal analysis of specimen M.1160.2 (Table III) may be explained by the occurrence of the rock in the unique current-bedded sequence at station M.1160. The high proportion of feldspar, low percentage of amphibole, pyroxene and rock fragments, and the absence of apatite were probably brought about by current sorting.

### *Depositional environment of the Annenkov Island Formation*

*Lower Tuff Member*

The regularity and evenness of the bedding and the predominance of laminated tuffaceous mudstone suggest deposition took place in fairly deep water below the influence of wave action. Thin, often lensoid, laminae of tuffaceous material were probably formed by the intermittent winnowing action of gentle bottom currents. The preservation of delicate articulated fish skeletal elements is also indicative of undisturbed sedimentation. The fauna (with the exception of trace-fossil burrows) was rich in planktonic forms, Radiolaria being particularly abundant. The tuffaceous material in the laminae and the disseminated pyroclastic elements in the mudstones were probably introduced by ash falls.

Interbedded tuffs, consisting of varying proportions of lithic crystal and vitric material of sandstone grade are frequently graded and often rest with an erosive contact on the underlying mudstones. This suggests that many of the tuffs were deposited by turbidity currents, probably initiated in areas of unstable accumulation nearer to the volcanic centre. Some of the tuffs, which lack the basal erosive contact, were probably deposited by direct pyroclastic fall-out.

A comparable succession has been described by Mitchell (1970, p. 212) from South Malekula in the New Hebrides. The rocks of the Lower Tuff Member are similar to his facies "C" of interbedded graded sandstones and mudstones. However, the absence of primary organic limestone and associated benthonic fauna suggests that the Annenkov Island rocks were probably deposited in deeper water than were the sediments of South Malekula.

*Upper Breccia Member*

The pattern of sedimentation of the Lower Tuff Member was abruptly interrupted by the influx of large quantities of coarse clastic material of andesitic derivation. The coarse, poorly sorted debris, the large scale of the sedimentation units of breccia and the erosive contacts between successive units all suggest deposition by mass-flow processes. The breccias exhibit many of the features characteristic of lahars (Fisher, 1960, p. 127), including lack of sorting, mixing of lower contacts, lack of vesicular and pumiceous fragments, the occurrence of broken mineral fragments and a small proportion of rounded clasts. Mitchell considered that his structureless rudites (facies "E" of the South Malekula Miocene succession), which from his description and photograph (Mitchell, 1970, p. 216, fig. 8) appear to be similar to the breccias of Annenkov Island, originated as subaërial lahars or mud flows which continued to flow down-slope after entering the sea (Mitchell, 1970, p. 218).

However, the Annenkov Island breccias show several important differences when compared with true lahars. Whereas the rudites (? lahars) of South Malekula are frequently interbedded with other lithologies (cf. Mitchell, 1970, fig. 5), the Annenkov Island rocks have comparatively few interbedded units of mudstone and those that do occur tend to be small and discontinuous. It is also debatable whether lahar deposition could produce an unbroken sequence of breccias such as the 200 m thick succession of south-western Annenkov Island (Fig. 13).

Another volcaniclastic succession of Miocene age from Espiritu Santo in the New Hebrides (Jones, 1967, p. 1281) has a much closer resemblance to the Annenkov Island succession. The Espiritu Santo succession consists of a 2 000 m thick clastic pile of predominantly unsorted and poorly sorted volcaniclastic rudites with locally abundant arenites and siltstones. The description of the lava rudites and the field relationships between rudites, arenites and siltstones (Jones, 1967, pl. 1 and 2) compares very closely with those of the lithologies on Annenkov Island. Unlike the Annenkov Island deposits, the Espiritu Santo rocks contain a small proportion of pumiceous material and, like the Malekula breccias, often include large proportions of organic clastic reef limestones.

Jones interpreted the Espiritu Santo clastic sequence as being the product of a marine andesite volcano and it is suggested that the Annenkov Island volcaniclastic sequence had a similar origin.

The steep flanks of a marine andesitic volcanic cone would presumably be composed of freshly erupted flow units together with pyroclastic debris. Such accumulations would be particularly unstable and liable to large-scale slumping, and submarine gravitational sliding would distribute thick unsorted accumulations of volcaniclastic material over a localized area adjacent to the volcanic cone. It is inferred that processes such as these were responsible for the deposition of the coarse structureless units of breccia on Annenkov Island. Copious amounts of volcaniclastic sandstone mixed and interbedded with the breccias can be interpreted as the product of attrition of the volcano when it built up to or above sea-level. A volcanic cone of newly erupted material is particularly vulnerable to marine erosion (Richards, 1960, p. 59), which, balanced by the continuing addition of erupted material, can produce vast quantities of sand and pebbly material. This would subsequently add to the instability of the cone and thus contribute to the sedimentation of associated coarser materials taking place in the vicinity of the eruptive centre. The paucity of vesicular and vitric pyroclasts may indicate derivation of the clastic material from fragmented flow units of lava or from debris erupted under submarine conditions where vesiculation was suppressed. The discontinuous mudstone units interbedded with the volcaniclastic sediments probably represent periods of quiescence when little or no material was erupted and the volcano became stable. Renewed activity probably resulted in further mass-flow deposition with partial destruction and disruption of the previously deposited mudstones. Innumerable intrusions of andesite within the Upper Breccia Member reinforces the idea of deposition in the close vicinity of a volcanic centre (see later discussion).

## Igneous Rocks

With the exception of two occurrences of spilite, all of the igneous rocks exposed on Annenkov Island and Hauge Reef are intrusive. There are two main groups:

i. Spilitic lavas and sills, which can be subdivided on the basis of petrography.
ii. A calc-alkaline assemblage of andesites and quartz-microdiorites probably related to some quartz-diorites collected from the Pickersgill Islands during the botanical landings of 1972–73.

Five occurrences of spilite were recorded from Annenkov Island and Hauge Reef. Of these, three exhibit intrusive contacts with the Lower Tuff Member and, of the two within the sequence of volcaniclastic breccias, one at least was extruded subaqueously and possesses poorly developed pillow structures. Field and thin section evidence suggests that the associated sedimentary rocks were only partially consolidated when the intrusive spilites were emplaced.

Of the calc-alkaline rocks, the andesites are by far the most abundant of any of the igneous rocks occurring on Annenkov Island and, although field relations are often exceedingly complex and difficult to interpret, all of the andesites are apparently intrusive. The majority of these intrusions are into volcaniclastic breccias (Upper Breccia Member) with which they are mineralogically identical. Field relationships indicate that, as with the intrusive spilites, the intrusions are broadly contemporaneous with the volcaniclastic sedimentary rocks which they intrude. Stock-like intrusions of quartz-microdiorite into the Lower Tuff Member are exposed on two islands of Hauge Reef. These show a petrographic similarity to the quartz-diorites collected from the Pickersgill Islands and it is possible that the quartz-microdiorites and quartz-diorites are the plutonic expressions of contemporaneous volcanism as represented by the andesites and andesitic volcaniclastic rocks which are exposed on Annenkov Island.

### *Spilitic lavas and sills*

The Annenkov Island spilitic rocks probably represent a small part of the much larger spilitic and basaltic assemblage exposed on the south coast of South Georgia. These were briefly studied by Trendall (1959), who subdivided them into "massive" and pillow lavas. He suggested that all the "lavas" were related to each other, some being extruded subaqueously whereas others may have been intruded as sills close to the submarine surface.

The spilitic rocks of Annenkov Island and Hauge Reef can be subdivided petrographically into three types which are characterized by the following mineral assemblages:

i. Phenocrysts of augite and pseudomorphic phenocrysts set in a groundmass of calcic and albitic feldspars with subordinate augite.
ii. Phenocrysts of oligoclase, relict labradorite and altered augite set in a groundmass of oligoclase and andesine.
iii. Oligoclase and accessories only.

*Type 1*. The spilites of this type occur as sills within the Lower Tuff Member at stations M.1152, 1153, 1163 and 1164.

In the cliffs and foreshore at stations M.1152 and 1153, a sill is exposed in the zone of disturbance related to a major fault. It occurs near the base of the thin-bedded tuffs and mudstones of the Lower Tuff Member. The field relationships of the sill to the adjacent sediments are clearly displayed in the cliffs at station M.1152. Because of the faulting, the sill has been brecciated and deeply weathered, and the adjacent sedimentary rocks have been crumpled. Apart from the tectonic disturbance, the upper contact of the sill is very uneven and at several points large protuberances of igneous rock cut cleanly across the bedding of the country rocks. Where seen, the lower contact exhibits a concordant relationship with the sediments. The sill can be traced in the cliffs towards the north-west to the landing beach (M.1153) used by Rustad and Trendall, where it forms the top of the natural arch figured by Holtedahl (1929, fig. 33). It is poorly exposed high in the cliffs next to the natural arch where brecciation of the sill is again related to the major fault. Although much of the sill is well exposed on the foreshore, its contacts with the country rocks are obscured by beach material. However, the dip of the country rocks between the cliff and the foreshore exposures indicates that the two exposures of the sill represent one igneous body. It was here that Trendall (1959, p. 23) recorded amygdaloidal lavas alternating repeatedly with tuffs. However, field mapping indicates that no lavas are present. It is therefore clear that Trendall misidentified the two exposures of the sill as separate lava flows.

A group of sills crops out in the same succession approximately 360 m above the intrusion described above. These sills, which branch and coalesce repeatedly along their line of outcrop, are exposed on the north-eastern coast (M.1163) and also about 0.5 km inland and to the south at approximately the same stratigraphical position (M.1164). The field data are summarized in Figs 16 and 17.

At station M.1163, two sills, when followed northward from their first appearance high in the cliffs, branch into three. One of these sills peters out and the remaining two coalesce into a single sill 6–7 m thick. Inland, and to the south (M.1164), the sills branch from three to a maximum of four. West of this station, the sills appear to terminate abruptly. Field mapping demonstrates that the overall stratigraphical position of this branched sill complex does not detectably change in the 0.5 km between the two stations where it is exposed. Although the intrusions appear to be restricted within comparatively narrow stratigraphical limits, local contacts between sill and country rocks are discordant. These irregularities are often related to changes in thickness, sometimes involving the amalgamation of adjacent sills.

Contacts with the sedimentary rocks are well exposed at stations M.1163 and 1164. Little or no chilling is apparent at the margins of the intrusions but in a zone approximately 15 cm in width the surrounding mudstones have been baked.

In the outcrop the spilites are frequently weathered to a depth of 10 cm on surface exposures and along joints. The unaltered rocks are greyish green in colour, grading to yellow-brown when weathered and they are further characterized by dark green spots (1–3 mm) identifiable in thin section as composite pseudomorphs. These superficially resemble amygdales and it is possible

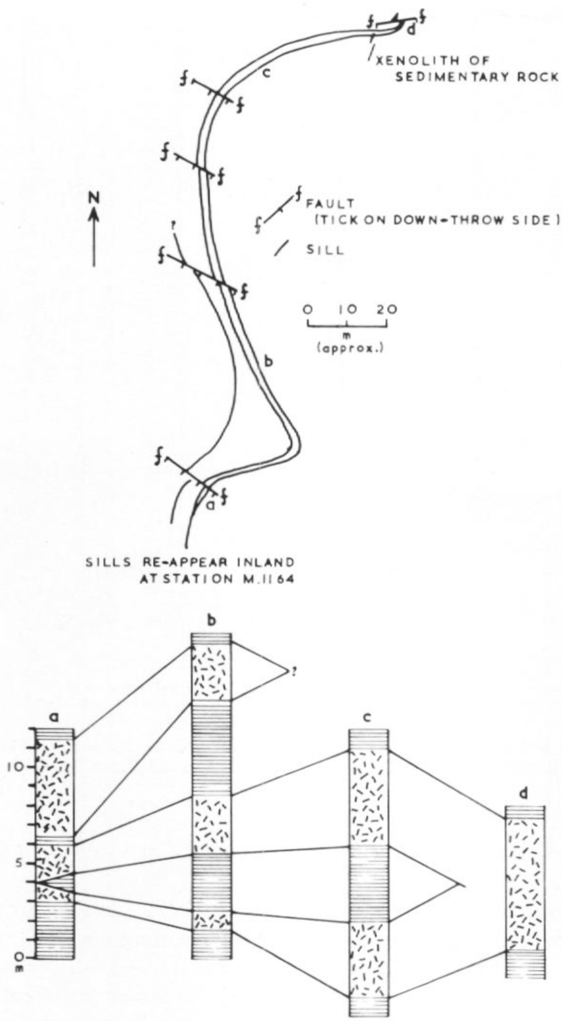


Fig. 16. Geological sketch map and sections illustrating the lateral variations in a group of spilitic sills on the north-east coast of Annenkov Island (M.1163).

that Trendall (1959, p. 23), when referring to amygdaloidal lavas on Annenkov Island, misidentified them as such.

The spilites primarily consist of sericitized oligoclase associated with subordinate augite and pseudomorphs, probably after olivine or orthopyroxene (Fig. 18c).

The oligoclase ($An_{20}$) occurs as intergrown laths (0.02–0.2 mm) showing straight extinction. Some of the laths are strongly zoned from a calcic core (approximately $An_{58}$) to a margin of oligoclase. Interspersed throughout the groundmass are interstitial pools and anhedral patches of fresh untwinned albite-oligoclase. With one exception, this variation in feldspar composition is evident in all of the specimens collected from the sills. However, in the vicinity of a small xenolith of interbedded mudstone and tuff (M.1163.13c), the igneous rock is basaltic in composition, the feldspars consisting of fresh labradorite ($An_{54}$). There is no textural difference between the basaltic part of the sill and the adjacent spilites either in the hand specimen or in thin section.

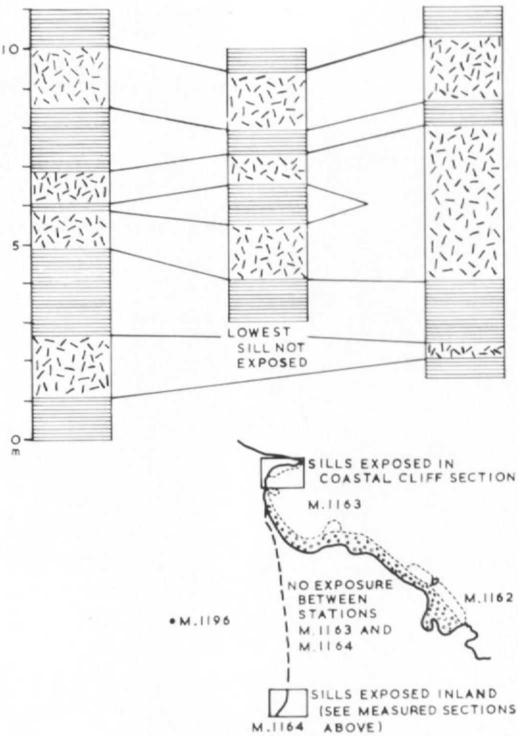


Fig. 17. Sections illustrating the development and lateral variations of the spilitic sills inland at station M.1164. The two insets show the locations where the sections reproduced in this figure and in Fig. 16 were measured.

Other samples from the centre and margins of the intrusion, when seen in thin section, contain oligoclase as described above.

In the feldspathic groundmass are set euhedral to anhedral crystals and crystal aggregates of fresh augite (0.03–1.0 mm; $\gamma: c = 45°$), often exhibiting zoning and the characteristic hour-glass structure. Larger, partially resorbed crystals of augite (1.0–3.0 mm) occasionally occur and possibly they represent an earlier generation of pyroxene crystallization. Towards the sill margins, both the pyroxenes and the feldspars are fluxionally arranged parallel to the contacts with the adjacent sediments, indicating that crystallization probably took place prior to and during intrusion.

Large composite pseudomorphs (0.3–3.0 mm), probably after orthopyroxene, are a conspicuous feature of the spilites both in the hand specimen and in thin section (Fig. 18c). These pseudomorphs, which have the form of prismatic, euhedral to subhedral crystals and crystal intergrowths, are composed predominantly of two mineral phases. The first is a colourless mineral occurring as fibres and lamellar aggregates; the fibres are usually arranged parallel to the direction of elongation of the pseudomorph. Their birefringence is low (white to pale yellow of the first order) and the lamellae individually give biaxial negative interference figures. Under high magnification (× 600), some of the fibres appear to be composed of fibrils, showing parallel extinction, trending obliquely across the fibres. These features indicate that the mineral is serpentine.

Intimately associated with the serpentine is a second pale green mineral of lamellar habit sometimes exhibiting faint pleochroism and with a high birefringence (0.021). This is bowlingite, which in some of the rocks sectioned occurs to the exclusion of the serpentine. Thin sections of

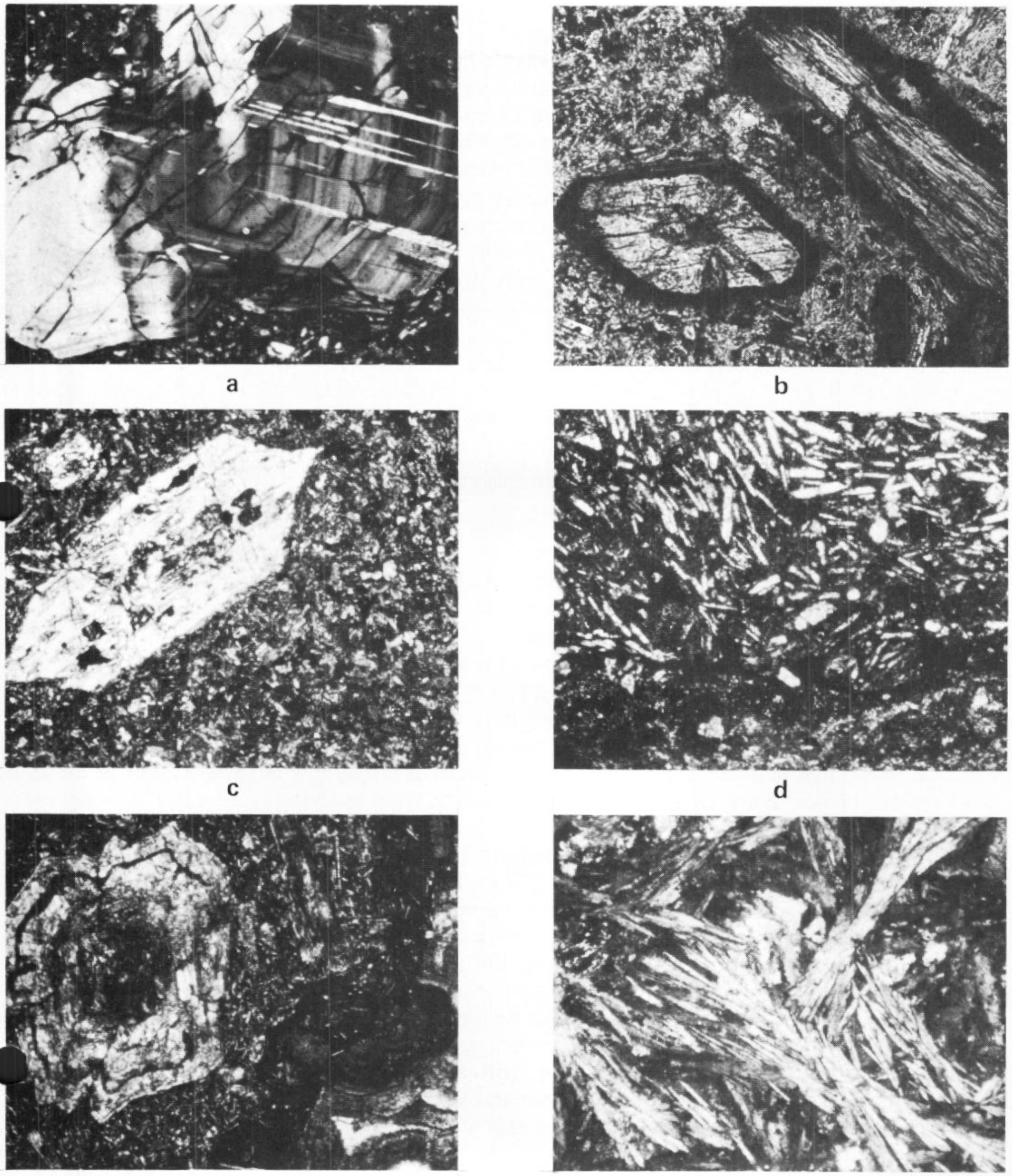


Fig. 18. a. An oscillatory zoned phenocryst of plagioclase in an andesite clast from a structureless breccia unit (M.1159.4c; X-nicols; × 25).

b. Hornblende phenocrysts marginally altered to magnetite in an andesite clast, Upper Breccia Member (M.1160.1; ordinary light; × 100).

c. Spilite (type 1). A pseudomorph of serpentine and bowlingite (after olivine or orthopyroxene) set in a groundmass of sericitized oligoclase and augite (M.1163.12; X-nicols; × 25).

d. An irregular contact between spilite (above) and mudstones (below). Plagioclase phenocrysts are fluxionally arranged within the spilite, and along the sediment–spilite interface small "flames" of mudstone penetrate into the igneous rock (M.1164.28; ordinary light; × 25).

e. Spilite (type 2). Concentric bands of chlorite within a large patchily altered phenocryst of plagioclase is indicative of original oscillatory zoning. An amygdale shows a colloform development of calcite, chlorite and ores (M.1195.2; ordinary light; × 25).

f. Spilite (type 3). Crystals of oligoclase exhibit a sub-variolitic texture (M.1174.1; X-nicols; × 100).

weathered rocks reveal that the bowlingite has oxidized to a yellow-brown lamellar substance with a high birefringence, partially obscured by its absorption colour. This is probably iddingsite, which is apparently often formed as an alteration product of bowlingite (Wilshire, 1958). Other minerals within the pseudomorphs include irregular patches of calcite, granules of opaque iron ore, chlorite and small chloritized flakes of biotite.

It is difficult to distinguish between the accessory and secondary minerals. Calcite, occurring in irregular patches (0.1–0.7 mm), and chlorite are probably secondary. Opaque iron ores in the form of small granules and cubes (0.03–0.13 mm), together with small amounts of biotite and acicular apatite are probably accessory minerals. Biotite is especially characteristic of the intrusion at stations M.1152 and 1153, where small subhedral flakes between 0.03 and 0.3 mm in length show partial alteration to chlorite.

A thin section of the spilitic rocks exposed on the foreshore at station M.1153 (M.1153.6a) exhibits a small vein 1.3 mm in width consisting mainly of intergrown laths and anhedral untwinned crystals of albite-oligoclase (0.3–0.7 mm in length), chloritized biotites, mossy aggregates of chlorite and abundant acicular apatites (up to 0.8 mm in length). Adjoining the vein is an (?) amygdale with an infilling of prehnite and zeolite. This vein would appear to represent a late-stage magmatic segregation.

The contacts between the sills and the country rocks are often markedly irregular in thin section. Such a contact is shown by specimen M.1164.28a, where "flames" of mudstone protrude into adjacent spilitic rock (Fig. 18d). This suggests that intrusion took place prior to consolidation of the sediments. Small mudstone xenoliths, usually no more than 2 mm in size, are often scattered sporadically along the sill margins.

Apart from occasional clastic feldspars and pyroxenes, in thin section it is difficult to resolve the mineral asemblages of the fine-grained mudstones adjacent to the sills. However, under high magnification they display a granoblastic texture consisting largely of intergrown feldspar and (?) quartz. The clastic feldspars are often turbid, probably because of recrystallization. Some anhedral feldspathic patches are consistently characterized by a low refractive index and biaxial positive interference figure, and may be albite resulting from recrystallization of originally more calcic plagioclase.

Recrystallization (contact metamorphic) effects are shown by a xenolith of sediment within a basaltic facies of the sills at station M.1163. This xenolith, which is approximately 10 cm long, is lozenge-shaped and consists of mudstone with an interbedded tuff. Absence of any angularity in its shape suggests that the sediments were unconsolidated when incorporated into the intrusion. The basalt adjacent to the xenolith is composed of small granular biotite crystals ($\sim$ 0.013 mm) surrounding laths of labradorite with lesser amounts of augite and pseudomorphs of bowlingite-iddingsite after (?) orthopyroxene. The mudstone part of the xenolith is generally fine-grained but it is peppered by large amounts of granular opaque iron ores, probably magnetite. Amorphous patches of the same appearance occur in the igneous rock adjacent to the xenolith and these are interpreted as originally patches of unconsolidated sediment derived from the xenolith. Narrow tongues of sediment protruding into the igneous rock from the xenolith are clearly visible in the hand specimen and in thin section, and these are a further indication that the sediments were unconsolidated during the intrusion process.

Associated with the magnetite grains in the mudstones, other minerals of metasomatic or contact metamorphic origin occur either as discrete crystalline clots or as small pod-shaped segregations. These consist of intergrown anhedral crystals of fresh albite associated with acicular and prismatic apatite and with a small amount of biotite. The latter is also sparingly dispersed throughout the matrix. These segregations are similar in mineralogy to the late-stage veining described above as occurring within the spilitic sill exposed at station M.1153.

The tuff interbedded with the mudstone in the xenolith has also been recrystallized. The fine-grained matrix between the grains contains large amounts of granular magnetite and subordinate biotite. The tuff consists predominantly of lava fragments, pumices, feldspars and augite.

Individual feldspars and feldspars within the andesitic rock fragments are turbid and exhibit uneven extinction. Biotites within the feldspars indicate that metasomatic alteration has occurred. The pumices exhibit a microscopic granoblastic texture and the clastic augites have altered margins peppered with magnetite.

*Factors governing the intrusion of spilitic sills.* Examples of intrusive spilitic rocks have been described by Benson (1915, p. 123 and 129), who concluded that nearly all of his spilites at Nundle represented shallow intrusions. Wells (1923) discussed several examples of intrusive spilitic pillow lavas and concurred with the view that they were emplaced as shallow intrusions into unconsolidated sediments.

McBirney (1963) considered that an ascending column of magma rising through an accumulating sedimentary sequence would, when encountering unconsolidated water-saturated sediments near the submarine surface, reach a point where extensive sill intrusion would be favoured rather than further upward migration and subaqueous extrusion. He also suggested that the lithostatic pressure of sediment and water overlying a magma above its critical temperature would inhibit vesiculation and hence facilitate retention of water. This, in turn, would increase the fluidity and therefore the lateral extent of any sills. Taking into account the temperature distribution in water-saturated sediments intruded by igneous sills (Jaeger, 1959), McBirney concluded that the chilling effects of such sills on wet sediments would be confined to a thin contact zone characterized by baking and dilation.

The spilitic sill complex exposed at stations M.1163 and 1164 is concordant. It is suggested that at the time of intrusion the level at which the complex is developed was at a critical depth below the submarine surface and the sediments were at least partially unconsolidated. The physical parameters were thus optimum for horizontal rather than vertical intrusion from a rising column of basaltic magma. During intrusion localized transgression and branching of the sills were favoured by the weak unconsolidated nature of the sediments; however, the sills could not deviate significantly from the confines dictated by the hydrostatic conditions. The sill rocks are predominantly non-vesicular and all the observed contacts are characterized by comparatively narrow zones of baked sediment. These features are also in accordance with the predictions made by McBirney.

*Type 2.* The spilites of this type are exposed at stations M.1154 (Hauge Reef) and M.1195 on Annenkov Island.

At station M.1154, a spilitic sill has been intruded into mudstones of the Lower Tuff Member exposed in a coastal cliff section (Fig. 21). The contacts of the sill are markedly discordant and along one of these lower discordant contacts the sediments are slightly deformed. This may indicate that the sediments were incompletely consolidated when they were intruded by the sills.

A spilite of identical petrography crops out over a small area south of station M.1195 on Annenkov Island. Only the lower contact of this is visible, making it difficult to determine whether it has an intrusive or extrusive origin. Because it is much more amygdaloidal than the spilite at station M.1154, it is probably extrusive. The area of outcrop is no more than 70 $m^2$ and it is bounded by scree and exposures of volcaniclastic breccias. It is therefore comparable in area of outcrop to the penecontemporaneously eroded pillow lava of station M.1174 described below. The spilite is underlain by mudstones dipping at 36° to the north-west.

In the hand specimen the spilites of this assemblage are dark green in colour. They have a porphyritic texture with microphenocrysts of altered plagioclase and augite set in a comparatively fresh aphyric groundmass. Amygdales of calcite are especially abundant at station M.1195. Weathering at the surface and along joints has produced brown limonitic crusts.

In thin section, severely altered phenocrysts of labradorite and augite are set in a fresher groundmass of plagioclase laths, dendritic opaque iron ores and chlorite (Fig. 18e).

The plagioclase phenocrysts (0.13–1.5 mm) have undergone albitization. They are subhedral to anhedral in form and albite twinning on partially unaltered crystals indicates an original labradoritic composition ($An_{54}$). However, most of the phenocrysts show partial to complete replacement by albite-oligoclase with associated calcite and chlorite. Apart from the amygdales, most of the calcite in the rock is closely associated with the altered feldspar and augite phenocrysts. The chlorite is often strikingly arranged in concentric bands within the feldspar phenocrysts, a feature which may be related to original oscillatory zoning (Fig. 18e). Small amounts of magnetite and epidote are also occasionally present within the altered phenocrysts.

The acicular groundmass feldspars (0.02–0.07 mm) are fresher than the phenocrysts and are andesine in composition ($An_{44}$). However, some of the feldspars exhibit compositional zoning from an andesine core to a marginal composition of oligoclase. The augite phenocrysts ($\gamma{:}c = 51°$) are subhedral to anhedral in form, 0.19–3.30 mm in length and, like the plagioclase phenocrysts, have been severely altered to calcite and chlorite. Crystals in various stages of alteration are present in a single thin section. Incipient alteration has occurred along crystal margins and fractures within the phenocrysts, whereas complete alteration has produced irregular pseudomorphs of calcite and chlorite. The interstices between the groundmass feldspar laths are occupied by chlorite and dendritic magnetite. The amygdales consist predominantly of calcite in large interlocking crystals; associated bands of chlorite and haematitized magnetite granules show a colloform structure (Fig. 18e). Often the amygdales are surrounded by a halo of dendritic magnetite.

*Type 3*. This type is represented by a single occurrence of pillow lava interbedded with andesitic volcaniclastic breccias intermittently exposed at station M.1174. This lava is uneven in thickness, varying between 0.2 and 1.0 m, and it has obviously suffered penecontemporaneous erosion as fragments derived from it are easily recognizable in the overlying andesitic volcaniclastic breccias. This erosion was probably responsible for the localized outcrop of the lava which is traceable for a distance of only 20 m before it wedges out into the adjacent breccias. A pillow structure is poorly developed with individual pillows ranging between 2 and 20 cm in size.

In the hand specimen, the rock is dark grey in colour with conspicuous white amygdales of calcite (0.5 mm–1.0 cm in size).

In thin section the lava exhibits the texture of a typical spilite, consisting almost exclusively of acicular oligoclase (0.06–0.5 mm) and showing a sub-variolitic structure (Fig. 18f). Late-stage granular and dendritic magnetite occurs within the feldspars and in the interstices between them. Irregular patches of sphene, calcite and chlorite are also present in the spaces between the feldspars together with a small amount of epidote.

The numerous amygdales are usually filled with prismatic calcite. However, a vein interconnecting several of the amygdales (M.1174.1) has introduced quartz which has crystallized within the calcite and, in one instance, it forms a continuous envelope between the calcite and the wall of the amygdale. Many of the amygdales are surrounded by an opaque layer, presumably of magnetite, within which smaller amygdales of spherulitic chlorite occur.

*Petrogenesis*. A large number of reviews dealing with spilitic rocks tend to regard them as polygenetic derivatives of a parental basaltic magma. Vallance (1960), Turner and Verhoogen (1960) and Hyndman (1972) considered a complex scheme of petrogenesis involving differentiation, assimilation, metasomatism and metamorphism of original basaltic magma and leading by converging lines of descent to spilites. This polygenetic approach was fully expounded in a series of papers edited by Amstutz (1974). The occurrence of laumontite in the tuffaceous rocks associated with the spilites is indicative of zeolite-facies metamorphism. Irregular patches of relict calcic plagioclase in several of the spilites suggest that the sodic plagioclase has replaced original labradorite. These observations are in accordance with those of Coombs (1974), Vallance (1969) and Battey (1974), who have argued convincingly that most if not all spilites represent basalts which have been weakly metamorphosed and metasomatized under saline conditions.

*Andesites**

Numerous irregular and sill-like bodies of andesite have been intruded into the Upper Breccia Member and, to a much lesser extent, into the rocks of the Lower Tuff Member. The andesites and the locally derived volcaniclastic rocks are almost identical in mineralogy and lithology, and it seems probable that they are genetically related.

The intrusions vary widely in size; outcrop areas range from several square metres to over 160 000 $m^2$ and several of the bodies are at least 30 m thick.

Three small, closely grouped knolls of intrusive andesite, surrounded by solifluction debris, are closely grouped to the north of Fan Lake. Contacts with the adjacent Lower Tuff Member are not exposed and it is not clear whether the intrusions represent separate bodies or are part of a single sill, sheet or dyke. All of the other observed occurrences of intrusive andesite are within sequences of volcaniclastic rocks in the southern and central parts of the island.

Most of the volcaniclastic rocks into which the andesites have been emplaced are completely unstratified and the contacts of the intrusions are correspondingly irregular. However, several sills in the scarps below the ridge south of McPherson Crags and north-west of Lawther Knoll are 10–20 m thick and have been intruded along the contact between massively bedded volcaniclastic sandstones (overlying rocks of the Lower Tuff Member) and unstratified volcaniclastic breccias. Whereas the lower contacts with the stratified sandstones are concordant, the upper contacts with the unstratified breccias appear to be irregular, suggesting that the presence or absence of stratification may exercise a control on the form of the intrusions.

The only multiple intrusion observed occurs at station M.1189, where a large intrusion of grey andesite in volcaniclastic rocks has been intruded by smaller bodies of pink andesite varying in size from veins 1–2 cm in width to irregular sheets and large bodies 3–4 m across.

Although the margins and contacts of many of the intrusions are relatively free from assimilated material and are thus well defined in the field (Fig. 19), other intrusions are characterized by a xenolithic marginal facies consisting of unsorted angular fragments of andesitic derivation set in the andesitic matrix of the intrusion (Fig. 20). The contact of this marginal facies with the breccias proper is frequently impossible to distinguish as the porphyritic intrusive andesites become densely charged with identical crystalline material derived from the matrix of the breccias. A paucity of recognizable xenoliths of breccia or sandstone in the intrusions and a correspondingly high proportion of discrete "xenocrysts" and "andesite xenoliths" suggest that in many instances the breccias were largely unconsolidated and were readily disaggregated by the permeation and intrusion of the andesitic magma.

Some of the intrusions (especially those at station M.1167 and beneath McPherson Crags) are distinctly heterogeneous and appear to consist of irregular inclusions of andesite within andesite. These inclusions often have indefinite contacts with the surrounding andesite and it is impossible to determine whether they are normal xenoliths of clastic andesite, derived from the adjacent volcaniclastic rocks as described above, or whether they are cognate xenoliths derived from processes involving autobrecciation during intrusion.

Other cognate xenoliths, definitely not derived from the sedimentary rocks, consist of diorite usually composed of minerals identical to the phenocrysts within the andesites. These xenoliths vary in size from 1 cm to a maximum observed size of 20 cm in an intrusion at station M.1175.

Texturally, the andesites are strongly porphyritic, reddish to grey in colour with phenocrysts of plagioclase, pyroxene and amphibole set in a fine-grained matrix and they are identical to the clasts in the associated breccias of the Upper Breccia Member.

*There are many more intrusions of andesite in the Upper Breccia Member than shown in Fig. 2. The complicated field relations and close lithological similarity of intrusions and country rocks prevented accurate representation of all but the larger intrusions in areas of good exposure.

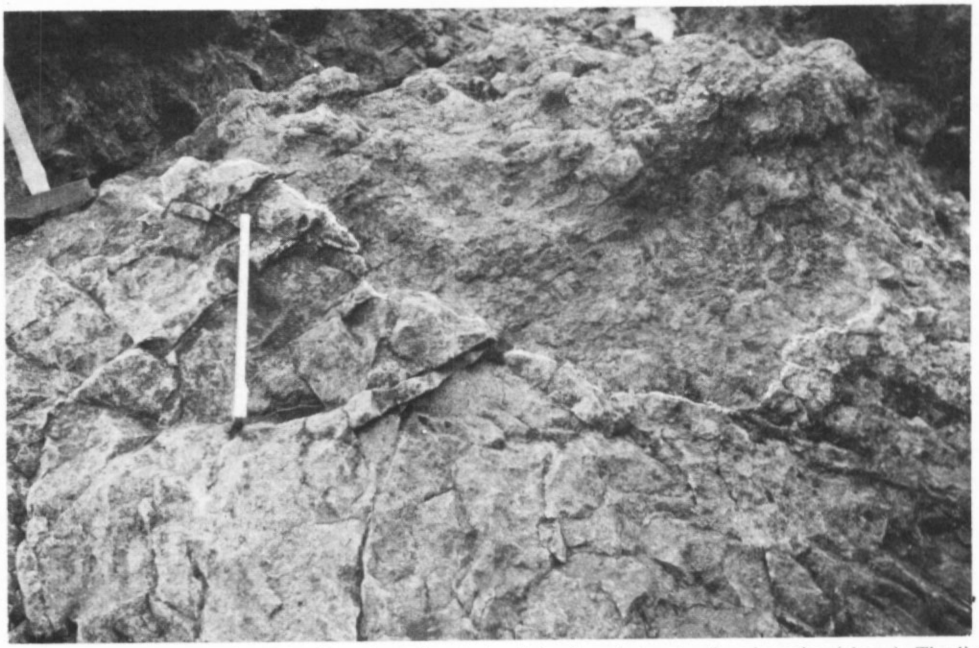

Fig. 19. Contact between an irregular intrusion of andesite (below) and structureless breccias (above). The line of contact has been marked with chalk. Foreshore section at station M.1157. The steel tape is 25 cm long.

In thin section most of the andesites are fresh, although some show alteration mainly in the form of zeolitization of the plagioclase phenocrysts and groundmass. The plagioclase phenocrysts (0.4–3.0 mm) are subhedral to anhedral in form and frequently exhibit strong compositional and oscillatory zoning from a labradorite core to an oligoclase-andesine margin. They are often sericitized and occasionally altered to calcite and zeolite.

Two varieties of amphibole phenocryst characterize the andesites. Common hornblende occurs as euhedral to subhedral crystals (0.02–3.0 mm; $\gamma{:}c = 18$–$20°$) often poikilitically enclosing plagioclase and lamprobolite (= basaltic hornblende; 0.02–2.5 mm; $\gamma{:}c = 10°$), which is slightly less abundant than the common hornblende but exhibits the same textural relationships. Normally, the two types of amphibole occur within the same intrusion and in some instances polyphase crystals consisting of both types clearly defined by their pleochroism are not uncommon. Many of the amphibole crystals exhibit varying stages of resorption. This ranges from a marginal peppering of the crystals to complete replacement by opaque magnetite (not to be confused with primary magnetite (see below)), in which case only the characteristic shape of the original amphibole is recognizable.

Subhedral to euhedral, pale green augite crystals, (0.15–1.00 mm; $\gamma{:}c = 54°$) are sparingly present in most of the intrusions, while biotite is a rare constituent in the form of individual lath-shaped crystals or in irregular aggregates associated with or enclosed within amphibole.

Apatite and iron ores occur as accessory minerals. The apatites are present as prismatic euhedral crystals often of comparatively large size (0.1–0.5 mm) and are commonly found within the mafic minerals especially near the margins of the amphiboles. In addition to being scattered throughout the matrix, magnetite occurs as inclusions within the mafic minerals.

The fine-grained groundmass and the feldspar phenocrysts often exhibit patchy alteration to zeolite, occurring as anhedral crystal patches and aggregates showing extinction parallel to a prominent cleavage. Haematitic iron ore is often associated with the zeolite, imparting a reddish

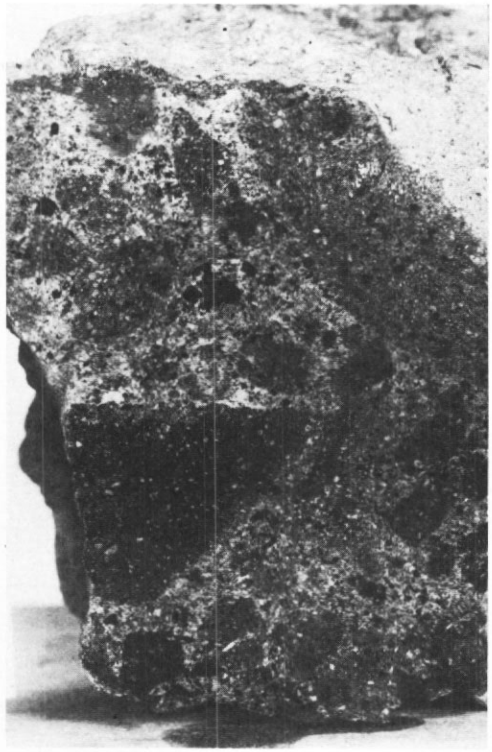

Fig. 20. Diffuse contact between intrusive andesite densely charged with xenoliths of andesite (below) and a volcaniclastic sandstone (above right) (M.1186.6). Natural size.

tinge to the rocks in the hand specimen. Slabs which were etched and stained with sodium cobaltinitrite indicated the presence of K-feldspar in the groundmass.

The dioritic cognate xenoliths are equigranular in texture with subhedral to anhedral crystals of plagioclase and common hornblende and/or lamprobolite often poikilitically enclosing the plagioclase. Augite is present in small amounts and sometimes shows an ophitic relationship towards the plagioclase. Apatite and magnetite occur as accessory minerals. The close mineralogical and textural relationship between the andesite and its contained medium- or coarse-grained xenoliths suggests that both phases crystallized from the same magma. Possibly, the xenoliths represent an initial period of cooling and partial solidification within a deeper magma chamber or chambers. Subsequent intrusion of the remaining magma into higher levels in the crust (carrying with it disrupted blocks from the initial phase of solidification) would result in faster cooling of the magma, ultimately producing an andesite containing the xenoliths and isolated phenocrysts.

*Quartz-microdiorites of Hauge Reef*

On the two islands of Hauge Reef which were visited (M.1154 and 1155, Figs 21 and 22) stock-like intrusions of quartz-microdiorite with associated "sheets" were found within rocks of the Lower Tuff Member.

At station M.1154 (Fig. 21), a cliff section (AB) exposes a large intrusion of quartz-microdiorite with a steep transgressive contact against sub-horizontal mudstones. The upper contact of the intrusion is not exposed. Along the section to the south, the intrusion appears to spread into a sheet, poorly exposed, near the top of the cliffs. The sheet is better exposed in cliff section CD

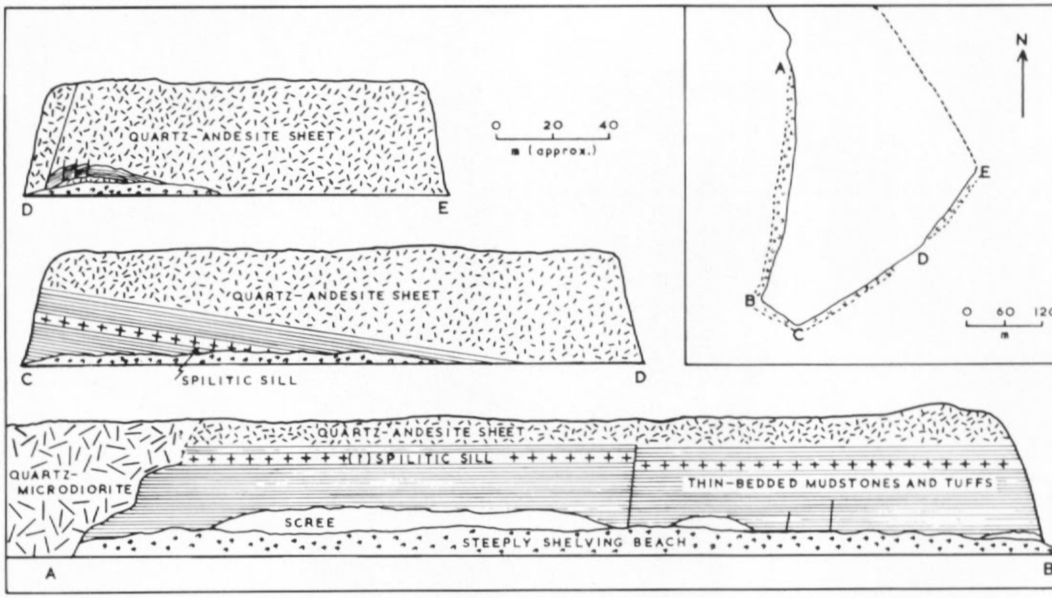


Fig. 21. Sketch map and sections illustrating the field relationships between the sedimentary and igneous rocks exposed on Hauge Reef (M.1154). All of the sections are approximately 30 m in height.

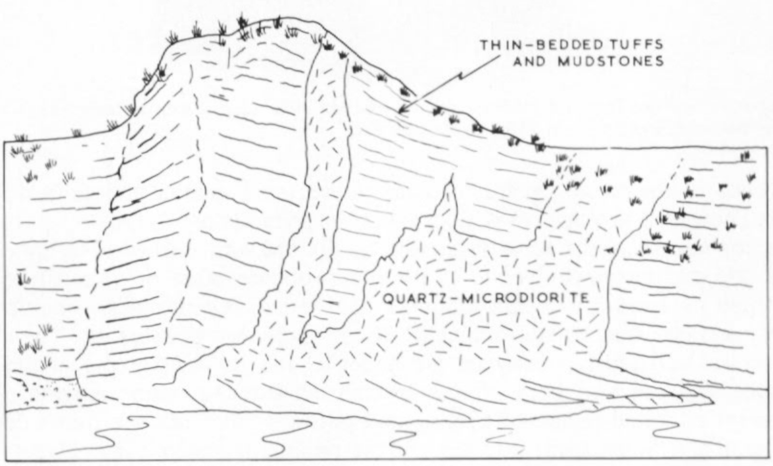


Fig. 22. A 30 m cliff section exposing an irregular intrusion of quartz-microdiorite into thin-bedded tuffs and mudstones. Coastal cliff section, Hauge Reef at station M.1155. (Drawn from photographs and a field sketch.)

(Fig. 21), where it is composed of a white fine-grained dacitic rock with plate-like crystals of mica aligned parallel to the contact with the sedimentary rocks.

There is another spectacular exposure of quartz-microdiorite in a 30 m high cliff section at station M.1155 (Fig. 22), where the upper part of an irregular stock-like intrusion is seen. This intrusion cuts cleanly across the sub-horizontal bedding of the surrounding mudstones with no apparent distortion of the latter or chilling at the contacts. Small xenoliths of country rock, restricted to the margins of the intrusion, suggest that the mechanism of intrusion was by stoping and assimilation.

The exposures of quartz-microdiorite on Hauge Reef show little variation in texture and mineralogy. In the hand specimen, abundant phenocrysts of white feldspar are set in a grey leucocratic groundmass; smaller amounts of biotite and amphibole are also present. The rocks are nowhere deeply weathered but they exhibit superficial rusty brown weathered surfaces.

In thin section, phenocrysts of plagioclase, hornblende and biotite are set in a groundmass consisting predominantly of anhedral plagioclase and quartz (Fig. 23a). Most of the rocks show signs of alteration. The plagioclase (0.05–3.3 mm) exhibits compositional and oscillatory zoning from a core of $An_{50}$ to a rim of $An_{20}$. The calcic cores of the feldspars are often highly sericitized and alteration to calcite along irregular cracks is also common.

Euhedral to subhedral hornblende (0.04–4.4 mm) shows partial to complete alteration to chlorite and calcite. Laths and foliaceous crystal aggregates of biotite (0.3–1.3 mm) are likewise altered to chlorite and some of the larger laths are intergrown with plagioclase.

Small euhedral phenocrysts of pleochroic (?) diopsidic augite (0.16 mm; $\gamma{:}c = 45°$) occur infrequently.

The groundmass consists of interstitial pools and patches of quartz (0.03–1.2 mm) intergrown with anhedral zoned plagioclase. The accessory minerals include subhedral apatite (0.06–0.5 mm) and irregular patches of opaque ore. Secondary calcite pervades the groundmass often in association with chlorite.

A thin section of the contact between igneous rock and mudstones at station M.1155 demonstrates that a fine-grained granoblastic texture has been imparted to the sediments by thermal metamorphism. Although difficult to resolve, the recrystallized components of the mudstones include anhedral quartz, aggregates of biotite and patches of opaque ore. Small veinlets of quartz occur in the mudstones and are sub-parallel to the contact with the igneous rock (Fig. 23b). The quartz-microdiorite immediately adjacent to the plane of contact contains abundant foliaceous biotite which may have been assimilated from the sediments. There is no sign of chilling at the intrusion margins.

The quartz-andesite sheet at station M.1154 is the fine-grained equivalent of the quartz-microdiorite. In the hand specimen it is greyish white in colour with numerous small dark brown plates of mica and white phenocrysts of plagioclase.

In thin section, the sheet appears as an unaltered leucocratic rock consisting of plagioclase phenocrysts in a fine-grained matrix of plagioclase, biotite and interstitial quartz. Unlike their counterparts in the quartz-microdiorites, the plagioclase phenocrysts (0.2–1.0 mm) consist of unzoned andesine ($An_{42}$), whereas the groundmass feldspars (0.06–0.1 mm) are oligoclase. Close to the contact of the sheet with the mudstones of the Lower Tuff Member, the plagioclase and biotite are fluxionally arranged. Thin plate-like crystals of biotite (0.1–2.0 mm) are often contorted, possibly because of movement through partially consolidated magma. Some of the biotites show marginal alteration to chlorite.

Small euhedral crystals of (?) diopsidic augite, identical to those found in the quartz-microdiorites also occur sporadically.

*Quartz-diorites of the Pickersgill Islands*

During a series of botanical landings on the southern side of South Georgia in the 1972–73 summer season, J. R. B. Tallowin collected several specimens from *in situ* outcrops of plutonic rock from the largest of the Pickersgill Islands. The field relations of these quartz-dioritic rocks are unknown but it is probable that they represent intrusions into sediments of Cumberland Bay type. Both in mineralogy and texture they are similar to the quartz-microdiorites of Hauge Reef.

In thin section, the quartz-diorites appear as fresh, mesocratic, equigranular rocks consisting of plagioclase, quartz, hornblende, biotite, augite and, in one specimen, hypersthene (Fig. 23c and d).

Most of the plagioclase occurs in the form of subhedral to anhedral interlocking crystals

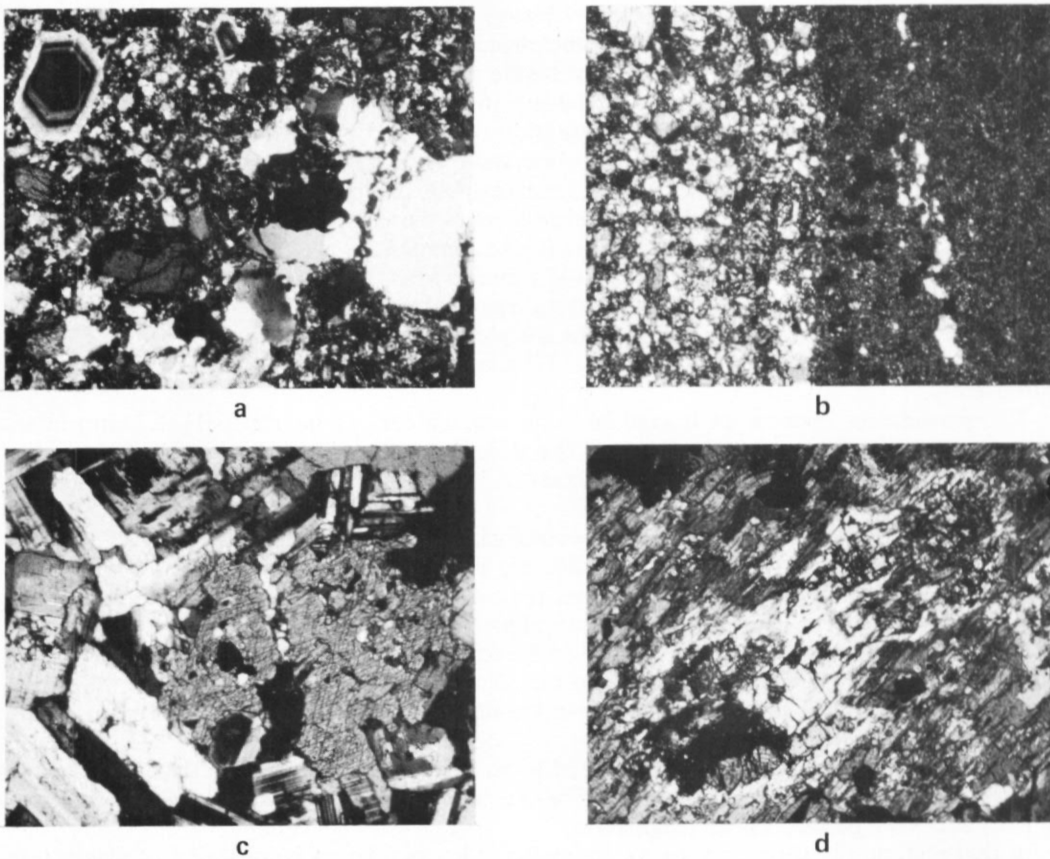


Fig. 23. a. Quartz-microdiorite showing strongly zoned plagioclase, subhedral hornblende and anhedral patches of quartz set in a felsic groundmass (M.1155.1; X-nicols; × 25).
b. Contact between quartz-microdiorite and mudstones. Small veins of quartz sub-parallel to the contact occur within the mudstones (M.1155.1; X-nicols; ×25).
c. Anhedral andesine, quartz, hornblende and biotite in a quartz-diorite from the Pickersgill Islands (M.1201.1; X-nicols; × 25).
d. Hypersthene with a thin mantle of augite enclosed by a large crystal of hornblende. Subhedral biotite crystals also occur within the hornblende (M.1201.1; X-nicols; × 25).

(0.1–3.0 mm) and exhibits strong compositional and oscillatory zoning from a labradoritic core to a margin of oligoclase. Unzoned crystals of andesine ($An_{42}$) are also present.

Large anhedral crystals of hornblende (0.1–4.0 mm; $\gamma{:}c = 34°$) frequently enclose crystals of anhedral biotite, plagioclase, augite, apatite, opaque ores and hypersthene (when the latter is present). The biotites contained in any one hornblende are frequently in optical continuity as are similarly occurring augite crystals.

Anhedral biotite (0.06–1.0 mm) commonly encloses plagioclase, augite, apatite and opaque ores.

Pale green anhedral crystals of augite (0.1–0.6 mm; $\gamma{:}c = 45°$), are rather sparse and tend to occur in close proximity to the other mafic minerals.

Altered remnants of pale pink pleochroic hypersthene (0.5–1.0 mm) were observed in two of the largest crystals of hornblende in a thin section of specimen M.1201.1. In one instance, a thin mantle of augite is developed between the enclosing hornblende and the ragged edges of the hypersthene (Fig. 23d). Hence, a reaction relationship of hypersthene → augite → hornblende is indicated.

Approximately 10% of anhedral quartz (0.1–1.6 mm) occurs in the interstices between the plagioclase and mafic minerals. Euhedral apatite (0.15–0.5 mm) and anhedral opaque ore (probably ilmenite) constitute the only accessory minerals.

## Regional Correlation

### *South Georgia*

The geology of South Georgia has been outlined by Trendall (1953, 1959). Flysch-type sedimentary rocks crop out over most of the island and on the basis of petrography he subdivided them into Cumberland Bay-type tuffaceous greywackes, composed of immature andesitic detritus derived from an island arc, and quartzose Sandebugten-type greywackes. The Cumberland Bay-type greywackes crop out over most of the island and have been thrust over the Sandebugten-type rocks, which are restricted in outcrop to the north-eastern side of South Georgia. Both sedimentary rock types have been strongly deformed and have a corresponding tectonic fabric. Abundant prehnite in rocks of Cumberland Bay type indicates low-grade (prehnite-pumpellyite facies) metamorphism (Skidmore, 1972).

Trendall (1953, p. 25) originally correlated the unfossiliferous Sandebugten-type sediments with the Palaeozoic Trinity Peninsula Series of Graham Land. The sparse fauna yielded by the Cumberland Bay-type rocks was considered by Wilckens (1937, 1947) as indicating a Cretaceous (Aptian) age. However, Casey (1961, footnote on p. 56) was of the opinion that some of the ammonites exhibited Neocomian and *not* Aptian affinities. *Belemnopsis* fragments collected from the northern coast of South Georgia are indicative of an Upper Jurassic–Lower Cretaceous age (Stone and Willey, 1973). In his second paper, Trendall (1959, p. 42) suggested that both sequences were Mesozoic in age but that a palaeogeographical change occurred between the deposition of the two types. Recent field work suggests that the two "types" were derived from differing provenances on opposite margins of the same basin (Dalziel and others, 1974, p. 293). Trendall (1959, p. 46) tentatively suggested that the axial trend of the basin receiving the sediments was east–west and that an island arc was located to the south of present-day South Georgia.

The sedimentary and igneous rocks of Annenkov Island, Hauge Reef and the Pickersgill Islands probably represent the remnants of such an island arc. The fossiliferous Annenkov Island Formation contrasts strongly with the coarser-grained flysch sequence on South Georgia and probably represents a shelf environment marginal to an island arc. The association of andesitic intrusions with coarse volcaniclastic deposits, such as would be expected to have accumulated in the close vicinity of an active submarine volcano, suggests that they may represent part of an eroded marine volcanic centre. It is possible that the granodioritic rocks of Hauge Reef and the Pickersgill Islands represent the plutonic equivalents of broadly contemporaneous calc-alkaline volcanism.

A plutonic igneous complex of gabbro, quartz-diorite and granite has been briefly described by Trendall (1959, p. 30) from the south-eastern extremity of South Georgia. Its field relationships with the adjacent Cumberland Bay-type sediments are complicated but Trendall suggested that the complex was paratectonic.

### *Southern Andean Cordillera*

The Yahgan Formation of the southern Andean Cordillera corresponds closely in lithology, age, metamorphic facies, tectonic fabric and vergence to the Cumberland Bay tuffaceous greywackes of South Georgia (Wilckens, 1933, p. 324; Katz and Watters, 1966, p. 341). The rocks are flysch deposits of greywacke facies and contain a large proportion of volcanic debris derived from an island arc. Fossils, including *Belemnopsis* (Hoffstetter, *in* Hoffstetter and others, 1957, p. 376) and *Inoceramus* (Katz and Watters, 1966, p. 326, fig. 7), may be similar to those from

South Georgia and Annenkov Island, respectively. Radiolaria are common in both sequences and the occurrence of the ammonite *Favrella* (Halpern and Rex, 1972, p. 1881) in rocks of the Yahgan Formation is indicative of a Lower Cretaceous (Neocomian) age in part for the formation. These rocks are also extensively prehnitized and are strongly overfolded towards the north. Basic suites consisting of sequences of highly altered basaltic and doleritic rocks associated with pillow lavas suggest large-scale contemporaneous magmatic activity (Katz and Watters, 1966, p. 342). Katz and Watters further suggested that these basic rocks are related to intrusive doleritic rocks of the pre-tectonic Dientes Sills emplaced at a different level into the sedimentary rocks. The overall evidence indicates that the Cumberland Bay-type rocks and the Yahgan Formation were deposited in the same basin (Suárez and Pettigrew, 1976) and this also favours the pre-continental drift position of South Georgia adjacent to the Andean Cordillera of South America (Hawkes, 1962, fig. 1; Dalziel and Elliot, 1973).

*Plate-tectonic interpretation*

*South Andean Cordillera.* Katz (1973) and Dalziel and others (1974, p. 291) considered the spatial relationships of the rock associations of the Andean Cordillera with a plate-tectonic interpretation of the geology and the following is a slightly modified synopsis of their work.

A discontinuous belt of mafic rocks (Rocas Verdes of Chilean geologists) extends along the length of the Andean Cordillera (between lat. 56° and at least lat. 51°S). This is flanked on the western side by the Patagonian granite batholiths (radiometrically dated as Upper Jurassic to Upper Cretaceous and younger). The Rocas Verdes are flanked on their eastern side by the Serie Tobifera (Quemodo Formation of Katz (1963, p. 507)), an Upper Jurassic sequence of subaerially erupted acid volcanic rocks. These overlie Palaeozoic basement and are, in turn, overlain in the east by marly-argillaceous marine sediments of a Lower Cretaceous age (Zapata Formation of Katz (1963)). Westward, sediments of the same age thicken into a flysch sequence rich in andesitic detritus (Yahgan Formation in part) overlying the basic assemblages of the Rocas Verdes. The basic rocks were intruded on a large scale up through the basement and the overlying acid volcanic rocks of the Tobifera Formation and are divisible into three zones:

iii. Subaqueously erupted basic (pillow) lavas fed by
ii. A sheeted dyke complex grading down into
i. A lowermost exposed zone of gabbro.

This assemblage thus represents development of oceanic crust between adjacent blocks of continental crust.

The widespread subaerial acid volcanicity of the Upper Jurassic Tobifera Formation is thought to be related to the initial separation of South America from Africa. Subduction probably began on the Pacific side of the Cordillera more or less simultaneously with the separation of the continents. Partial submergence of the subaerially erupted Tobifera Formation rocks on the western margin occurred in some places before the complete cessation of acid volcanicity (Katz, 1963, p. 508). In the eastern part of the submerged zone, the Tobifera Formation was overlain by the Lower Cretaceous Zapata Formation, while in the west submergence was immediately followed by large-scale intrusion and subaqueous extrusion of basic material (Rocas Verdes). This has been studied in detail at Sarmiento (Dalziel and others, 1974), where large volumes of basic material, intruded between continental blocks, grade progressively upwards from gabbro to sheeted dyke complexes to pillow lavas. This injection of basic material is interpreted as being related to back-arc sea-floor spreading behind an actively forming island arc with the consequent formation of a marginal basin. The Yahgan Formation type flysch sequence overlying "oceanic crust" consists predominantly of andesitic debris which increases westward towards the Patagonian Batholith, which is interpreted in part as the plutonic root of a Lower Cretaceous island arc (or arcs). Later, the arc was pushed back towards the continental margin with the resulting deformation of the sedimentary flysch infill of the basin.

*South Georgia*. A pre-drift reconstruction of South Georgia adjacent to the southern Andean Cordillera is favoured here. This would mean that the Cumberland Bay tuffaceous greywackes, together with the flysch deposits of the Yahgan Formation, represent a marginal basin fill adjacent to an island arc (or arcs). The arc is now represented in South Georgia by the southern volcanic belt including the quartz-dioritic rocks of Hauge Reef and the Pickersgill Islands and by the andesitic and volcaniclastic rocks of Annenkov Island (Suárez and Pettigrew, 1976). The quartzose Sandebugten-type rocks could have been derived from a Patagonian continental provenance.

A major problem in this plate-tectonic interpretation involves the closing of the basin and the folding and thrusting of the Cumberland Bay sequence over rocks of the Sandebugten type. On the south-western coast of South Georgia, north of Annenkov Island, the rocks are apparently only slightly deformed, whilst on Annenkov Island itself the rocks are undeformed and gently tilted. Furthermore, geophysical evidence indicates that the rocks of the volcanic belt underlying the continental shelf of South Georgia are likewise gently folded (personal communication from P. F. Barker). A similar structural pattern has been recognized in the southern Andean Cordillera (Suárez and Pettigrew, 1976) and thus it is difficult to reconcile the closure of the basin with a simple translation of the arc towards the continent as envisaged by Dalziel and others (1974, p. 294), in which case it would be expected that the degree of deformation would increase and not decrease in a southerly direction, i.e. towards the arc.

*Mechanism of marginal basin formation*. Mechanisms of marginal basin formation have been discussed by Karig (1971), Oxburgh and Turcotte (1971) and Packham and Falvey (1971). The generation of calc-alkaline magma on an island arc is related to the partial melting of oceanic crust on a descending slab of lithosphere along a subduction zone, the necessary heat being generated by friction at the upper margin of the descending plate. At deeper levels, friction along the upper surface of the slab is considered to produce convective instability in the overlying mantle with the consequent uprise of diapiric mantle material. This, in turn, causes crustal extension at or behind the island arc, which is thus translated away from the continent. Such extension will contribute to the arcuate form of the arc as it moves oceanwards.

Dalziel and others (1974, p. 294) deduced that a marginal basin formed in the southern Andes during a single intensive pulse of basic magmatism coeval with the initiation of the island arc. However, abundance of basic lavas, spilitic rocks and sills at comparatively high stratigraphical levels in the Yahgan Formation and at a considerable distance from the inferred position of the island arc (Katz and Watters, 1966; Suárez and Pettigrew, 1976) possibly indicates that crustal extension and corresponding basic magmatic activity related to the initial formation of the basin continued intermittently and on a reduced scale during deposition of the Yahgan Formation. Similarly, the abundance of basic extrusive/intrusive rocks along the south coast of South Georgia and the paucity of intermediate/acid flow units may also indicate similar late-stage basic magmatism unrelated to that of the island arc.

## CONCLUSIONS

A 10 000 year B.P. glaciation of South Georgia can probably be correlated with the extensive differential glacial erosion of Annenkov Island, the effects of which have been partially masked by subsequent periglacial erosion. Similarly, the 5 000 year B.P. glacierization of South Georgia can be equated with the formation of a small glacial valley with associated moraine.

A discontinuous platform around Annenkov Island at approximately 30 m above sea-level can be correlated in part with similar features developed on Hauge Reef and the coast of South Georgia. They probably represent former levels of marine erosion cut during isostatic re-adjustment after the 10 000 year B.P. glaciation of South Georgia.

Continuing isostatic elevation after recent glacial phases is suggested by the development of a present-day wave-cut platform associated with the lower-level raised beaches.

The sedimentary rocks of Annenkov Island were deposited in an environment bordering an island arc situated at the edge of a Lower Cretaceous marginal basin. The lower 860 m of tuffs and tuffaceous mudstones (Lower Tuff Member) exposed on Annenkov Island represent the effusive products of explosive calc-alkaline volcanicity. Disseminated, predominantly vitric pyroclastic materials present in most of the mudstones were introduced by direct ash fall. Graded beds of tuff were either deposited by ash fall and/or by turbidity currents initiated by the gravitational collapse of unstable accumulations of primary tuffaceous material in the immediate vicinity of a volcanic centre.

This pattern of sedimentation was virtually terminated by the submarine eruption of andesitic magma and the formation of an andesitic submarine volcano. Gravitational collapse and marine erosion of the volcano was balanced by the addition of newly erupted material, leading to the widespread distribution of coarse volcaniclastic sandstones and breccias. On Annenkov Island, these deposits are represented by a volcaniclastic succession, which is at least 1 000 m in thickness (Upper Breccia Member). Innumerable intrusions of andesite, identical in mineralogy and texture to the clastic material comprising the volcaniclastic succession, indicate deposition adjacent to the volcanic centre.

Rare basic lavas and sills in both formations are correlated with similar rocks exposed on Hauge Reef and the southern coast of South Georgia. These are probably the products of island-arc volcanicity, although they may represent diminutive late phases of magmatic activity connected with an earlier large-scale magmatic phase which occurred during the initiation of a marginal basin by back-arc sea-floor spreading.

The faulting and tilting of the Annenkov Island rocks may be coeval with late-stage faulting on South Georgia. During continental drift and the formation of the Scotia Sea, the continental block of South Georgia and Annenkov Island drifted eastward, away from South America, to its present position in the South Atlantic Ocean.

The geology of Annenkov Island is critical to an interpretation of the palaeogeographical conditions governing the deposition of the sedimentary rocks of South Georgia. It also has important implications for the positioning of South Georgia prior to continental drift and the subsequent formation of the Scotia arc. Geochemical studies and dating of the igneous rocks should establish the validity of correlations with similar geological assemblages in the southern Andean Cordillera.

## Acknowledgements

The field work for this paper was carried out with the assistance of E. G. Lawther, who did most of the plane-table work, and I. T. Bury. Drs R. J. Adie, M. R. A. Thomson and P. W. G. Tanner advised on the preparation of the manuscript, and I am grateful to members of the British Antarctic Survey in the Department of Geological Sciences, University of Birmingham, for much helpful discussion. Finally, I wish to thank Emeritus Professor F. W. Shotton and Professor A. Williams for the use of facilities in the Department of Geological Sciences, University of Birmingham.

*MS received 10 July 1975*

## REFERENCES

Adie, R. J. 1964. Geological history. (*In* Priestley, R. E., Adie, R. J. *and* G. de Q. Robin, *ed. Antarctic research*. London, Butterworth and Co. (Publishers) Ltd., 118–62.)

Amstutz, G. C., *ed.* 1974. *Spilites and spilitic rocks*. Berlin, Heidelberg, New York, Springer-Verlag. [International Union of Geological Sciences, Ser. A, No. 4.]

Barker, P. F. *and* D. H. Griffiths. 1972. The evolution of the Scotia Ridge and Scotia Sea. *Phil. Trans. R. Soc.*, Ser. A, **271,** No. 1213, 151–83.

BATTEY, M. H. 1974. Spilites as weakly metamorphosed tholeiites. (*In* AMSTUTZ, G. C., *ed. Spilites and spilitic rocks.* Berlin, Heidelberg, New York, Springer-Verlag, 365–72.)

BENSON, W. N. 1915. The dolerites, spilites and keratophyres of the Nundle District. *Proc. Linn. Soc. N.S.W.*, **40**, Pt. 1, 121–73.

CASEY, R. 1961. A monograph of the Ammonoidea of the Lower Greensand. Part 2. *Palaeontogr. Soc. [Monogr.]*, 45–118.

CLAPPERTON, C. M. 1971. Geomorphology of the Stromness Bay–Cumberland Bay area, South Georgia. *British Antarctic Survey Scientific Reports,* No. 70, 25 pp.

COOMBS, D. S. 1960. Lower grade mineral facies in New Zealand. *21st Int. geol. Congr., Norden, 1960,* Pt. 13, 339–51.

——. 1974. On the mineral facies of spilitic rocks and their genesis. (*In* AMSTUTZ, G. C., *ed. Spilites and spilitic rocks.* Berlin, Heidelberg, New York, Springer-Verlag, 373–85.)

CUMMINS, W. A. 1962. The greywacke problem. *Lpool Manchr geol. J.*, **3**, Pt. 1, 51–72.

DALZIEL, I. W. D. *and* D. H. ELLIOT. 1973. The Scotia arc and Antarctic margin. (*In* STEHLI, F. G. *and* A. E. M. NAIRN, *ed. The ocean basins and their margins. I. The South Atlantic.* New York, Plenum Publishing Corporation, 171–246.)

——., DE WIT, M. J. *and* K. F. PALMER. 1974. Fossil marginal basin in the southern Andes. *Nature, Lond.*, **250,** No. 5464, 291–94.

FISHER, R. V. 1960. Criteria for recognition of laharic breccias, southern Cascade Mountains, Washington. *Bull. geol. Soc. Am.*, **71,** No. 2, 127–32.

HALPERN, M. *and* D. C. REX. 1972. Time of folding of the Yahgan Formation and age of the Tekenika Beds, southern Chile, South America. *Geol. Soc. Am. Bull.*, **83,** No. 6, 1881–85.

HAWKES, D. D. 1962. The structure of the Scotia arc. *Geol. Mag.*, **99,** No. 1, 85–91.

HOFFSTETTER, R., FUENZALIDA, H. *and* G. CECIONI, 1957. Chile. (*In Lexique stratigraphique international. Vol. V. Amérique Latine,* Fasc. 7, 444 pp.)

HOLTEDAHL, O. 1929. On the geology and physiography of some Antarctic and sub-Antarctic islands. *Scient. Results Norw. Antarct. Exped.*, No. 3, 172 pp.

HORNE, R. R. 1968. Petrology and provenance of the Cretaceous sediments of south-eastern Alexander Island. *British Antarctic Survey Bulletin,* No. 17, 73–82.

——. *and* B. J. TAYLOR. 1969. Calcareous concretions in the Lower Cretaceous sediments of south-eastern Alexander Island. *British Antarctic Survey Bulletin,* No. 21, 19–32.

——. *and* M. R. A. THOMSON. 1972. Airborne and detrital volcanic material in the Lower Cretaceous sediments of south-eastern Alexander Island. *British Antarctic Survey Bulletin,* No. 29, 103–11.

HYNDMAN, D. W. 1972. *Petrology of igneous and metamorphic rocks.* New York, etc., McGraw-Hill Book Company.

JAEGER, J. C. 1959. Temperature outside a cooling intrusive sheet. *Am. J. Sci.*, **257,** No. 1, 44–54.

JONES, J. G. 1967. Clastic rocks of Espiritu Santo Island, New Hebrides. *Geol. Soc. Am. Bull.*, **78,** No. 10, 1281–87.

KARIG, D. E. 1971. Origin and development of marginal basins in the western Pacific. *J. geophys. Res.*, **76,** No. 11, 2542–61.

KATZ, H. R. 1963. Revision of Cretaceous stratigraphy in Patagonian Cordillera of Ultima Esperanza, Magallanes Province, Chile. *Bull. Am. Ass. Petrol. Geol.*, **47,** No. 3, 506–24.

——. 1973. Contrasts in tectonic evolution of orogenic belts in the south-east Pacific. *J.R. Soc. N.Z.*, **3,** No. 3, 333–61.

——. *and* W. A. WATTERS. 1966. Geological investigation of the Yahgan Formation (Upper Mesozoic) and associated igneous rocks of Navarino Island, southern Chile. *N.Z. Jl. Geol. Geophys.*, **9,** No. 3, 323–59.

KOHL-LARSEN, L. 1930. Die deutsche Südgeorgien-Expedition 1928/29. *Z. Ges. Erdk. Berl.*, 1930, Nr. 9–10, 321–50.

MCBIRNEY, A. R. 1963. Factors governing the nature of submarine volcanism. *Bull. volcan.*, Sér. 2, **26,** 455–69.

MITCHELL, A. H. G. 1966. Geology of South Malekula. *New Hebrides Condominium Geological Survey Report,* No. 3, 42 pp.

——. 1970. Facies of an early Miocene volcanic arc, Malekula Island, New Hebrides. *Sedimentology,* **14,** Nos. 3/4, 201–43.

——. *and* A. J. WARDEN. 1971. Geological evolution of the New Hebrides island arc. *J. geol. Soc. Lond.*, **127,** Pt. 5, 501–29.

NANZ, R. H. 1954. Genesis of Oligocene sandstone reservoir, Seeligson Field, Jim Wells and Kleberg Counties, Texas. *Bull. Am. Ass. Petrol. Geol.*, **38,** No. 1, 96–117.

OXBURGH, E. R. *and* D. L. TURCOTTE. 1971. Origin of paired metamorphic belts and crustal dilation in island arc regions. *J. geophys. Res.*, **76,** No. 5, 1315–27.

PACKHAM, G. H. *and* D. A. FALVEY. 1971. An hypothesis for the formation of marginal seas in the western Pacific. *Tectonophysics,* **11,** No. 2, 79–109.

PETTIGREW, T. H. *and* L. E. WILLEY. 1975. Belemnite fragments from Annenkov Island. *British Antarctic Survey Bulletin,* No. 40, 33–36.

PETTIJOHN, F. J., POTTER, P. E. *and* R. SIEVER. 1972. *Sand and sandstone.* New York, Springer-Verlag.

RICHARDS, A. F. 1960. Rates of marine erosion of tephra and lava at Isla San Benedicto, Mexico. *21st Int. geol. Congr., Norden, 1960,* Pt. 10, 59–64.

SKIDMORE, M. J. 1972. The geology of South Georgia: III. Prince Olav Harbour and Stromness Bay areas. *British Antarctic Survey Scientific Reports,* No. 73, 50 pp.

STEWART, R. J. 1974. Zeolite facies metamorphism of sandstone in the western Olympic Peninsula, Washington. *Geol. Soc. Am. Bull.*, **85,** No. 7, 1139–42.

STONE, P. 1974. Physiography of the north-east coast of South Georgia. *British Antarctic Survey Bulletin,* No. 38, 17–36.

——. *and* L. E. Willey. 1973. Belemnite fragments from the Cumberland Bay type sediments of South Georgia. *British Antarctic Survey Bulletin,* No. 36, 129–31.

Suárez, M. *and* T. H. Pettigrew. 1976. An Upper Mesezoic island-arc—back-arc system in the southern Andes and South Georgia. *Geol. Mag.,* **113,** No. 4, 305–28.

Trendall, A. F. 1953. The geology of South Georgia: I. *Falkland Islands Dependencies Survey Scientific Reports,* No. 7, 26 pp.

——. 1959. The geology of South Georgia: II. *Falkland Islands Dependencies Survey Scientific Reports,* No. 19, 48 pp.

Turner, F. J. *and* J. Verhoogen. 1960. *Igneous and metamorphic petrology.* 2nd edition. New York, Toronto and London, McGraw-Hill Book Company, Inc.

Vallance, T. G. 1960. Concerning spilites. *Proc. Linn. Soc. N.S.W.,* **85,** Pt. 1, 8–52.

——. 1969. Spilites again: some consequences of the degradation of basalts. *Proc. Linn. Soc. N.S.W.,* **94,** Pt. 1, 8–50.

Weeks, L. G. 1953. Environment and mode of origin and facies relationships of carbonate concretions in shales. *J. sedim. Petrol.,* **23,** No. 3, 162–73.

Wells, A. K. 1923. The nomenclature of the spilitic suite. Part II: The problem of the spilites. *Geol. Mag.,* **60,** No. 2, 62–74.

Wilckens, O. 1932. Fossilien und Gesteine von Süd-Georgien. *Scient. Results Norw. Antarct. Exped.,* No. 8, 28 pp.

——. 1933. Der Südantillen-Bogen. *Geol. Rdsch.,* **24,** 320–35.

——. 1937. Geologische Ergebnisse der Deutschen Süd-Georgien Expedition Dr. Kohl-Larsen 1928–29. *Geol. Rdsch.,* **28,** 127–28.

——. 1947. Paläontologische und geologische Ergebnisse der Reise von Kohl-Larsen (1928–29) nach Süd-Georgien. *Abh. senckenb. naturforsch. Ges.,* No. 474, 66 pp.

Wilshire, H. G. 1958. Alteration of olivine and orthopyroxene in basic lavas and shallow intrusions. *Am. Miner.,* **43,** Nos. 1 and 2, 120–47.

Zen, E-an. 1961. The zeolite facies; an interpretation. *Am. J. Sci.,* **259,** No. 6, 401–09.